Neurobiology of Disease 55 (2013) 44–62

Contents lists available at SciVerse ScienceDirect

Neurobiology of Disease

journal homepage: www.elsevier.com/locate/ynbdi

PKC activation during training restores mushroom spine synapses and memory in the aged rat

Jarin Hongpaisan *, Changqing Xu, Abhik Sen, Thomas J. Nelson, Daniel L. Alkon

Blanchette Rockefeller Neurosciences Institute at West Virginia University, Morgantown, WV, 26505, USA

ARTICLE INFO

Article history:
Received 17 July 2012
Revised 14 March 2013
Accepted 19 March 2013
Available online 29 March 2013

Keywords:
Aging
PKC
Synapse
Dendritic spine
Hippocampus

ABSTRACT

Protein kinase C (PKC) ε and α activation has been implicated in synaptogenesis. We used aged rats to test whether the PKCε/α activator bryostatin and PKCε-specific activator DCP-LA combined with spatial memory training could restore mushroom dendritic spinogenesis and synaptogenesis. Compared with young rats, aged, learning-impaired rats had lower memory retention; lower densities of mushroom spines and synapses in the apical dendrites of CA1 pyramidal neurons; fewer PKCε-containing presynaptic axonal boutons; and lower activation and expression of two PKCε/α substrates, the mRNA-stabilizing protein HuD and brain-derived neurotrophic factor (BDNF). PKC activator treatment combined with spatial memory training restored mushroom spines and mushroom spine synapses; rescued PKCε/α expression and PKC/HuD/BDNF signaling; and normalized memory to the levels seen in young rats. These effects were produced by treatment with either bryostatin or the PKCε-specific activator, DCP-LA. Bryostatin also reversed alterations in GABAergic inhibitory postsynaptic currents (IPSPs) in aged, learning-impaired rats. Thus, our results support the therapeutic potential of PKC activators when added to cognitive rehabilitation for inducing mushroom spine synaptogenesis and reversing memory decline associated with aging.

Introduction

In humans, the most common age-related cognitive dysfunction is impaired spatial memory (Nilsson, 2003; Uttl and Graf, 1993; Wilkniss et al., 1997). Spatial memory in humans involves the hippocampus (Shrager et al., 2007), and the right hippocampus in particular is important for the recall of spatial location (Smith and Milner, 1981). Several groups have described changes in dendritic spine morphology and synaptic density in the dorsal hippocampus (Miranda et al., 2006; Moser et al., 1994; Rusakov et al., 1997) – particularly the generation of mushroom spines and synapses within CA1 pyramidal neurons (Hongpaisan and Alkon, 2007) – that correlate with changes in spatial memory. Age-related cognitive decline also involves changes in spine structure and a loss of synaptic function (Calhoun et al., 1998; Govoni et al., 2010; Hof and Morrison, 2004; Phinney et al., 1999; Rapp and Gallagher, 1996), and age-associated electrophysiological and morphological changes at the synapse have been described (Burke and Barnes, 2006; Lister and Barnes, 2009; Wilson et al., 2006; Xu et al., 2009).

Under healthy conditions, memory-specific activation of protein kinase C (PKC) in dendritic regions of the mammalian hippocampus is important for memory retention (Bank et al., 1988; Olds et al., 1989). There is an abundance of PKCε in presynaptic nerve fibers, which supports its role in neurite outgrowth, synapse formation, and neurotransmitter release (Shirai et al., 2008). PKCε directly affects the actin cytoskeleton and promotes neurite outgrowth (Prekeris et al., 1996), is crucial for synaptic formation (Hama et al., 2004), and stimulates expression of brain-derived neurotrophic factor (BDNF) essential for synaptic stability (Sun et al., 2008). In humans and animals, a decrease in PKC activity has also been observed in the aging brain at the level of the whole hippocampus, suggesting that a role for PKC in the neurobiology of aging (reviewed by Battaini and Pascale, 2005; Govoni et al., 2010). Van der Zee et al (2004) reported changes in specific PKC isozymes at the neuronal cell level in the hippocampal CA1 stratum oriens in aged rats.

PKCε and PKCα are known to activate the nuclear export and transport of the HuD protein into the dendrites and axons (Hongpaisan and Alkon, 2007; Pascale et al., 2005). HuD is a member of the embryonic lethal, abnormal vision, *Drosophila* (ELAV)-like Hu proteins, which are involved in mRNA post-transcriptional stability through binding to AU-rich elements (AREs) in the 3′-untranslated regions (3′-UTR) of target transcripts (Antic and Keene, 1998; Chung et al., 1997; Pascale et al., 2004, 2005; Quattrone et al., 2001). HuD is expressed only in neurons and localizes to both pre- and postsynaptic sites (Akten et al., 2011; Hongpaisan and Alkon, 2007). HuD binds a number of neuronal transcripts, including growth-associated protein-43 (GAP-43) and neurofilament-M (Perrone-Bizzozero and Bolognani, 2002), and has been shown to regulate neurite outgrowth and dendritic spine and

* Corresponding author at: Blanchette Rockefeller Neurosciences Institute, 8 Medical Center Drive, Morgantown, WV 26505-3409, USA. Fax: +1 304 293 7536.
E-mail address: jhongpaisan@brni.org (J. Hongpaisan).
Available online on ScienceDirect (www.sciencedirect.com).

0969-9961/$ – see front matter © 2013 Elsevier Inc. All rights reserved.
http://dx.doi.org/10.1016/j.nbd.2013.03.012

synapse formation (Aranda-Abreu et al., 1999; Hongpaisan and Alkon, 2007).

PKC activators have been shown to enhance cognitive function and improve memory during normal aging (see Govoni et al., 2010 for review). Bryostatin (bryostatin 1) is a macrolide lactone and a powerful PKC agonist that activates both conventional PKC (e.g., PKCα) and novel PKC (e.g., PKCε) isozymes at nanomolar concentrations (Mutter and Wills, 2000). The binding of bryostatin to PKC results in PKC translocation to the plasma membrane and activation. Bryostatin-bound PKC is then downregulated by ubiquitination and proteasomal degradation. Downregulation of PKC is significant with high and/or prolonged concentrations of bryostatin (Matthews et al., 1997). In mice, i.v. injection of bryostatin (40 μg/kg) leads to a brief, nanomolar level increase of bryostatin in the brain that is sufficient to activate its targeted PKC isozymes, followed by a rapid decrease in the brain. The same dose of bryostatin administered to mice by i.p. injection leads to a much lower peak brain level, but a sustained increase in bryostatin levels in the brain compared with i.v. injection (Zhang et al., 1996).

We have previously shown that treatment of young, healthy rats with the PKC activator bryostatin during spatial learning enhanced recent memory and increased the number of mushroom dendritic spines and formation of mushroom spine synapses (Hongpaisan and Alkon, 2007). In the present study, we assessed the ability of treatment with the PKCα and PKCε activator bryostatin or the PKCε-specific activator 8-[2-(2-pentyl-cyclopropylmethyl)-cyclopropyl]-octanoic acid (DCP-LA), in addition to water maze training, to reverse age-related biochemical and morphologic changes in hippocampal spines and synapses and to restore recent spatial memory in aged rats. Specifically, we characterized changes in PKCε and PKCα levels and signaling in the dentate gyrus/CA3/CA1 pathways of the hippocampal circuit at the level of single neurons and axonal boutons; morphologic changes in single dendritic spines and synapses; and electrophysiological changes at the level of single neurons in the right dorsal hippocampus of young and aged rats after water maze training, with or without PKC activator treatment. We then correlated biochemical, histological, and electrophysiological changes with improvement in learning and recent memory.

Material and methods

Animals and PKC activators

Brown Norway rats were obtained from the National Institute on Aging (NIA), National Institutes of Health (NIH) facilities at Harlan (Indianapolis, IN); approximately 108 rats were used to collect data in the present study. The number of animals used in each experimental condition was based on power analysis, previously calculated for similar studies in our lab: ≥10 animals for behavioral and electrophysiological studies, and ≥3 animals for biochemical and microscopic studies. This is also consistent with other researchers who used at least 3 animals in their studies, e.g. Nicholson et al. (2006), for electron microscopy. Animals were housed in our animal facility for 1 month prior to experiments. All research was carried out in accordance with the EU Directive 2010/63/EU for animal experiments. Bryostatin was kindly provided by the National Cancer Institute (NCI), NIH, Bethesda, MD. DCP-LA was synthesized at our institute (Blanchette Rockefeller Neurosciences Institute, Morgantown, WV; Nelson et al., 2009).

Water maze training and treatment

The effects of bryostatin and DCP-LA on spatial memory retention were studied in rats that had undergone water maze training, as follows. Rats were either 5 months old (young) or >24 months old (aged) on the first day of spatial memory training, with water maze training and drug treatment administered for approximately 21 days. At the end of the water maze training period, spatial memory was assessed in a probe test as previously described by Hongpaisan and Alkon (2007).

Briefly, young and aged rats were moved to the water maze room in their home cages at least 1 h before training in a water maze pool (152 cm in diameter and 60 cm high) filled with water at 22 ± 1 °C. At the beginning of each trial, a single rat was placed in the water facing the maze pool wall, using different starting positions for each trial, and allowed to swim until it found a hidden platform (15 cm × 15 cm) that was submerged approximately 2 cm below the surface of opaque water. Rats remained on the platform for 20 s and then were returned to their home cages. Rats that failed to find the platform within 120 s were guided to the platform by the investigator. The swim path was recorded with a video-tracking system that calculates time to find the platform, swim distance, and percentage of time spent in quadrants of the pool.

For each rat, the water maze trial was repeated 2 times per day for 5 days. Latency time, or the total time for the rat to reach the platform in each trial, was measured and compared across all trials to assess learning capacity over time. Aged rats that showed a rapidly declining latency time curve, with the average latency time within the mean ± 2 × SEM of that of young rats, were classified as aged, learning-unimpaired. Aged rats with a slower decline in the latency time curve, with the average latency time greater than the mean ± 2 × SEM of that of young rats, were classified as aged, learning-impaired.

Rats were administered bryostatin (5 μg/kg, i.p.) or drug vehicle every 48 h for 10 days starting 24 h after the end of water maze training (Supplemental Fig. 1A). Then, the rats underwent a second period of training (2 swims per day for 5 days), with bryostatin or drug vehicle treatment continuing through the end of the 2nd water maze training period. On days that treatment occurred on the same day as a swim test, rats were injected 30 min before the swim test. The same treatment regimen was used for DCP-LA (1.5 mg/kg, i.p.).

At 24 h after completion of the second water maze training, memory retention was determined by a spatial memory probe test, in which rats must swim to the target area, but with the platform removed. Video-tracking was used to assess movements in each quadrant during a probe test period of 1 min. The number of times the target area was crossed per minute was used as the measure of spatial memory. At 24 h after the probe test, or 48 h after the last water maze trial, the hippocampus of each rat was used to assess morphologic, molecular, and electrophysiological changes in dendritic spines and synapses.

Anesthesia

Rats were deeply anesthetized using chloral hydrate (Sigma-Aldrich, St. Louis, MO; 400 mg/kg body weight, i.p.) and the hippocampus removed for use in immunoblotting, immunohistochemistry, and electron microscopy as described below. For the electrophysiological study, rats were placed under isoflurane (Baxter, Deerfield, IL) sedation and then decapitated.

Immunoblot analysis

At 24 h after the probe test, rats were placed under deep anesthesia (chloral hydrate) and the right and left hippocampi were dissected and immediately frozen on dry ice. Total PKCε and PKCα were measured only in the whole right hippocampus, the area that has been shown to be important for spatial memory (Smith and Milner, 1981). The right hippocampus was lysed by sonication in homogenizing buffer containing 10 mM Tris–Cl (pH 7.4), 1 mM PMSF (phenylmethylsulfonyl fluoride), 1 mM EGTA, 1 mM EDTA, 50 mM NaF, 20 μM leupeptin, and 1% Triton-X 100. The homogenate

was centrifuged at 800 ×*g* for 15 min at 4 °C to obtain the soluble protein and concentration was measured using the Coomassie Plus (Bradford) Protein Assay kit (Pierce, Rockford, IL). 20 μg of protein was separated by SDS-PAGE on a 4–20% gradient Tris–Glycine gel (Invitrogen, Carlsbad, CA) and then transferred to nitrocellulose membrane, which was blocked with BSA at room temperature for 15 min and then incubated with primary antibody and mouse anti-β actin antibody (Santa Cruz Biotechnology, Santa Cruz, CA) overnight at 4 °C. The blots were then incubated with alkaline phosphatase conjugated secondary antibody (Jackson Immunoresearch Laboratories, West Grove, PA) at 1:10,000 dilution for 45 min, and developed using the 1-step NBT-BCIP substrate (Pierce). Immunoblots were imaged with ImageQuant RT-ECL (GE Life Sciences, Piscataway, NJ) and densitometric quantification was performed using IMAL software (Blanchette Rockefeller Neurosciences Institute). PKCε and PKCα levels were quantified by double blind analysis (unknown treatment of hippocampal sample) and normalized to the beta-actin protein level.

Confocal microscopy

Rats were deeply anesthetized with chloral hydrate and perfused through the heart by gravity with phosphate buffered saline (PBS) for <4 min at room temperature. Rats were then perfused with 4% paraformaldehyde in PBS at room temperature to remove any negative impact of hypothermia on the number of dendritic spines (Kirov et al., 2004). Although the blood wash-out period was short, we noticed that the fixative that left the circulation at the opened right atrium was red in color, yet these animals were fixed as effectively as those perfused with a longer wash-out period. In addition, we did not find macroscopically any blood clots in the meningeal blood vessels when we removed the brain from the skull of fixed animals. Under confocal microscopy, we also did not find auto-fluorescence of red blood cells. These observations suggested that formaldehyde, which we used for perfusion, could diffuse through plasma membrane and immediately fix blood cells and other blood coagulant proteins, after which the blood cells are continuously expelled from the blood circulation during fixative perfusion.

Brains were then removed, postfixed for 10 min, and stored in PBS at 4 °C. Right dorsal hippocampi were dissected and sectioned at 35 μm thickness with a vibratome (Leica VT1000S). A series of sections, kept in PBS at 4 °C, were selected from the right dorsal hippocampus starting at approximately 2400 μm and selecting 1 section every 600 μm and then processed for various confocal microscopy studies as described below. In order to make quantitative comparisons in immunohistochemistry across experimental groups, sets of animals from each experimental condition and controls were perfused on the same day, the tissues sectioned and processed for immunohistochemistry using the same reagents, and the slices imaged using the same confocal microscopy parameters on the same day.

Hippocampal slices were oriented with a Zeiss Axio Observer Z1 microscope equipped with a 710 confocal scanning system using the 10× objective lens in the DAPI channel (for staining nuclei). The random CA1 or CA3 area that appeared immediately after switching to the higher magnification lens, either 63× or 100× Plan-APO Chromat oil immersion objectives (1.4 NA), was imaged for appropriate fluorescence (e.g., Alexa 488 and/or 568), used for quantification. Confocal images of hippocampal sections were acquired in line scan mode with a pinhole of approximately 1.00 Airy unit and averaged data from several images were reported. Confocal images with similar levels of DAPI fluorescence intensity among experimental conditions were quantified with the ImageJ program (http://rsb.info.nih.gov/ij/). Control data were set at 100%, and all other experiment data were defined as % of their controls.

Immunohistochemistry

As previously described (Hongpaisan and Alkon, 2007), hippocampal slices of 35-μm thickness were incubated free-floating overnight at room temperature with primary antibodies: rabbit polyclonal anti-PKCε (1:100; Millipore/Upstate, Billerica, MA); mouse monoclonal anti-PKCα (1:100; Millipore/Upstate); mouse monoclonal anti-brain derived neurotrophic factor (BDNF; 1:50; Santa Cruz Biotechnology); mouse monoclonal anti-synaptophysin (1:2000; Millipore); mouse monoclonal anti-growth-associated protein (GAP)-43/B-50 (1:2000; Millipore/Chemicon); polyclonal anti-spinophilin (1:100; Millipore/Upstate); and polyclonal anti-neurogranin (1:400; Millipore/Chemicon). Tissue sections were then incubated with either Alexa Fluor 568 goat anti-rabbit (1:200; Invitrogen/Molecular Probes) secondary antibody for 3 h at room temperature, or biotinylated anti-mouse (1:20; Vector Laboratories, Burlingame, CA) secondary antibody for 3 h at room temperature and then streptavidin-conjugated Alexa Fluor 488 (1:100; Invitrogen/Molecular Probes) for 3 h at room temperature. Sections were mounted with VECTASHIELD mounting medium with DAPI to counterstain nuclei (Vector Laboratories). For negative controls, primary or secondary antibody was replaced with protein with no antigenicity against the tested antibody.

Two to three confocal images of CA1 stratum radiatum and 2 images of pyramidal neuron cell bodies in the stratum pyramidale were randomly collected from each hippocampal section, 4 hippocampal sections (approximately 600 μm apart along the dorsal hippocampus) per rat. Therefore, a maximum of 10 CA1 stratum radiatum and 8 stratum pyramidale areas was taken from each rat, unless hippocampal sections were folded, torn, or damaged.

Densities of pre- and postsynaptic structures

After immunohistochemical processing, we measured the densities of postsynaptic dendritic spines (spinophilin grains), presynaptic axonal terminals (synaptophysin grains), postsynaptic membranes (neurogranin grains), and presynaptic membranes (GAP-43 grains) per $63 \times 63 \times 0.6\ \mu m^3$ volume of the CA1 stratum radiatum (where apical dendrites of CA1 pyramidal neurons are located). Images were analyzed by grain counting using the ImageJ program, with procedures similar to those described in the South Carolina Algal Ecology Lab online notebook (http://www.dnr.sc.gov/ael/notebook/imagej_counts/counts.html). In brief, the 8-bit gray scale images were inverted, so that the dark pixels became light and vice versa. The (light) background of the photographic negative was then subtracted, using a background subtraction command, in order to omit diffuse, low-fluorescence staining of proteins that had not yet been transported to pre- and postsynaptic structures. The images were converted from an 8-bit (256 shades of gray) to a 1-bit (black or white) image. The particles that ended up touching one another were then processed for separation. Only particles within the range of pixel sizes of the measured structures were defined and counted.

Relative tissue shrinkage/swelling

Confocal microscopy and morphometry were used to compare whether neurons/tissue from young and aged brains experienced differential shrinkage/swelling after histological preparation. We determined the density and volume of DAPI-stained nuclei of CA1 pyramidal neurons within a randomly selected area of the CA1 stratum pyramidale in selected sections after immunohistochemical staining and counterstaining with DAPI. The density of pyramidal neurons was counted in 3 random areas of the CA1 stratum pyramidale, from 4 hippocampal sections (approximately 600 μm apart along the dorsal hippocampus) per rat (total 12 areas/rat).

3D reconstruction analysis of dendritic spine morphology on dendritic shafts

Fresh tissue sections were stained with 1,1′-Dioctadecyl-3,3,3′,3′-tetramethylindo-carbocyanine perchlorate (DiI; Molecular Probes/Invitrogen) to determine the number of distinct shapes of dendritic spines on individual dendritic shafts, as described previously (Hongpaisan and Alkon, 2007). The tips of glass electrodes, prepared for electrophysiological experiments, were immersed 2–3 times for 10 s in 5% (w/v) DiI in dichloromethane (Sigma-Aldrich) and air-dried at room temperature for 1 h. The tips of DiI-coated electrodes were inserted, broken, and left in the strata oriens of the CA1 area of hippocampal sections at 150 μm thickness (3–4 electrode tips/slice). After maintenance in PBS at 4 °C overnight to allow DiI to diffuse into the plasma membrane of CA1 neurons, hippocampal sections were resectioned to 35 μm thickness and mounted on glass slides, using distilled water as a mounting medium. Dendrites stained with DiI (>510 nm/568 nm; excitation/emission) were imaged by confocal scanning microscopy using 100× Plan-APO Chromat oil immersion objective (1.4 NA). A series of randomized confocal images (1024 pixels × 1024 pixels) were confocally scanned at every 0.145 μm. According to Nyquist sampling, a pixel size was 48, 48, and 145 (x, y, and z in nm). Three-D confocal images were deconvoluted by 10 iterations of the Richard–Lucy algorithm using a freely available ImageJ plugin, Deconvolution Lab (Biomedical Imaging Group, EPFL; Lausanne, Switzerland). A confocal stack of point spread function used for deconvolution was prepared from Fluoro-max dyed red aqueous fluorescent beads (63 nm diameter, 1% w/v stock solution; Thermo Scientific, Fremont, CA); further diluted to 1:10,000, smeared, and air-dried on a microscopic slide coated with 0.01% poly-L-lysine. Dendritic spines were automatically detected and counted with a freely available NeuronStudio (beta) program (Rodriguez et al., 2008). Dendritic projections from dendritic spine shafts at 0.2–3 μm length were classified as dendritic spines, and dendritic spines with a head diameter larger than 600 nm were considered to be mushroom dendritic spines (Sorra and Harris, 2000).

Four hippocampal sections (approximately 600 μm apart along the dorsal hippocampus) per rat were stained with DiI. Each hippocampal section was placed with 3–4 tips of DiI-coated glass. From 0 to 3 dendritic spines could be imaged with confocal microscopy in the CA1 stratum radiatum area, adjacent to each DiI-coated glass tip.

Synaptic density

The density of synapses was evaluated by electron microscopy, as modified from Harris et al. (1992) and Hara et al. (2012), to confirm the dendritic spine density determined with DiI staining and immunohistochemistry. For electron microscopy, chloral hydrate-anesthetized rats were perfused through the heart (5 s) with PBS and then with 2% glutaraldehyde and 3% paraformaldehyde in PBS. Brains were removed and stored in fixative at 4 °C. Similar to confocal microscopy, series of hippocampal sections, kept in PBS at 4 °C, were selected from the right dorsal hippocampus starting at approximately 2400 μm and selecting 1 section every 600 μm. Hippocampal slices at 70 μm thickness were processed for Epon-embedding and resectioned on the 70-μm thick surface to 90 nm (0.09 μm) thickness. A ribbon of serial sections was collected on a grid and stained with uranyl acetate and lead citrate. Electron micrographs were taken of the middle of each section to avoid compression at the periphery of the section with a Zeiss Libra 120+ electron microscope. Random sampling to determine synaptic density was achieved by orienting the hippocampal CA1 area under low-power magnification. To avoid large proximal apical dendrites close to cell bodies of CA1 pyramidal neurons (stratum pyramidale), electron micrographs were taken from the CA1 stratum radiatum approximately 200–250 μm from the cell bodies, where synapses are evenly distributed throughout the micrographs. The random area that immediately appeared after switching to a higher magnification (5000× magnification and a pixel resolution of 266.859 pixels/μm) was imaged with a CCD camera (UltraScan, Gatan, Pleasanton, CA), and the adjacent areas were taken from its serial sections. For each rat, electron micrographs of serial-section sets were collected: 4 serial-section sets per hippocampal section (or <4 in cases of tissue folding, overlapping, or damage) from 4 hippocampal sections (approximately 600 μm apart along the dorsal hippocampus). During quantification, serial sections of electron micrographs taken at 5000× magnification (5 × 5 μm^2 CA1 stratum radiatum area) were digitally zoomed to 20,000× magnification to help identify the pre- and post synaptic structure details, by using the default program Preview on a MacPro 4.1 computer with a 30-inch monitor (Apple, Cupertino, CA). We defined axospinous synapses as those located between dendritic spine structures that do not contain mitochondria and with axon boutons containing presynaptic vesicles. Synaptic density was collected within a 5 × 5 × 0.09 μm^3 of the CA1 stratum radiatum of a central section, using adjacent 2–3 sections above or under the central section (total of 5–7 sections in 1 serial-section set) to define the morphology of dendritic spines and location of the synapses in the central section. In addition, we did not measure the density within the whole serial section volume to avoid uncertain morphology of dendritic spines and their synapses in the peripheral sections that were not seen in the central section. Quantitative classification of dendritic spines as "mushroom" spines required that spine "heads" have a cross-sectionally visualized diameter of >600 nm (Harris et al., 1992; Sorra and Harris, 2000) as measured from the reference or adjacent section with maximal spine head diameter in ImageJ. The morphology of macular and perforated PSDs of mushroom spine synapses was identified from the serial sections. Dendritic spines with diameter less than 600 nm were counted as thin and stubby spines together. The morphology of macular and perforated postsynaptic densities (PSDs) on mushroom spines was identified from the serial sections. The density of all axospinous synapses reflected the density of all synapses on mushroom, thin, and stubby dendritic spines. Increased numbers of presynaptic vesicles in axon boutons were measured as an increase in the frequency of axon boutons with presynaptic vesicles that occupied more than 50% of the cross-sectional space not occupied by other organelles.

Electrophysiological recordings

As previously described (Xu et al., 2009), hippocampal slices (250–300 μM) from rats decapitated under isoflurane sedation were perfused with artificial cerebrospinal fluid heated to 30–33 °C at a rate of 2–3 ml/min. CA1 pyramidal cells were identified visually by using an Axioskop 2FS microscope (Zeiss) equipped with a 40× water-immersion objective coupled with an infrared differential interference contrast camera system. With whole-cell patch-clamp recordings, membrane current and potential signals were digitized and analyzed with Digidata 1322A and pClamp 8.2 systems (Molecular Devices). Patch pipettes of ≈5 MΩ were pulled with a Narishige PP-830 puller (Narishige, Greenvale, NY). The diffusion potential (liquid junction potential) was 4 mV calculated by Clampex software. Under these conditions, synaptic currents were acquired at a holding potential of −70 mV, the high concentrations of chloride in the pipette caused the IPSC to appear as an inward current. QX314 was added to the pipette solution to block the $GABA_B$-mediated currents and to prevent the generation of Na^+-dependent action potentials. Spontaneous excitatory amino acid currents (sEPSCs) were excluded from recordings by adding glutamate receptor antagonists DNQX (6,7-dinitroquinoxaline-2,3-dione) and AP5 (DL-2-amino-5-phosphonovaleric acid); therefore, all of the recorded inward currents were sIPSCs. The method of recording inhibitory synaptic currents was set up according to the methods described by Rodriguez-Moreno et al (2000), with some adjustments.

$GABA_A$-mediated inward currents were recorded with whole-cell electrodes containing high concentrations of chloride and 1 mM QX314 using the continuous single-electrode voltage-clamp mode. Access resistance (<25 MΩ) was regularly monitored during

recordings and cells were rejected if resistance changed >15% during the experiment. If the access resistance increased during the course of the experiment and caused significant reductions in the synaptic current amplitudes, efforts were made to improve access (such as applying additional suction or slight positive pressure); if this failed, the experiment was discontinued. Spontaneously occurring synaptic currents were filtered at 2 kHz and digitized at 10 kHz using Digidata 1322A. Synaptic currents were collected at 60 s for each experimental condition. Off-line analysis of synaptic currents was performed using the Minianalysis software (Version 6.0; Synaptosoft, Decatur, GA). Synaptic currents were screened automatically using an amplitude threshold of 3 pA. Events were then visually screened to ensure that the analysis was not distorted by changes in noise level or by membrane fluctuations. If the background noise increased during the recording, the data from that cell were discarded. The data generated from these measurements were used to plot cumulative probability amplitude and interevent interval graphs, with each distribution normalized to a maximal value of 1. Cumulative probability plots obtained under different experimental conditions were compared using the nonparametric Kolmogorov–Smirnov (K–S test), which estimates the probability that two cumulative distributions differ from each other by chance alone (Wu et al., 2002). The significance level for the K–S test was set at a value of $P < 0.05$. Sources of all chemicals are described in Xu et al. (2009).

Data and statistical analysis

Measurement was performed with blinded analysis in the following experiments: 1) Immunoblot — the researcher did not know the age or the treatment of each hippocampal sample; 2) Dendritic spine morphology (DiI staining) and synaptic density (electron microscopy) — the researcher did not know the age and treatment of each confocal image or electron micrograph. All samples were labeled by J.H. with a code that was not known by the researcher who did the measurement. After all samples were quantified, data were decoded and calculated for statistical analysis. Data from the blinded analyses were used to confirm the data from confocal immunohistochemistry and electrophysiology experiments, which were not performed with blinded analysis.

All data are shown as mean ± SD in text and tables and as means ± SEM in all figures, with n = the number of measurements, as detailed in Tables 1 and 2. All data were first statistically probed by one-way ANOVA. Behavioral data with a statistically significant overall difference among the groups by ANOVA were then further analyzed for between-group differences (e.g., maze vs. maze plus bryostatin) with one-way ANOVA. The data from confocal and electron microscopy, immunoblot, and electrophysiology studies that showed a significant overall difference among the groups by ANOVA were further analyzed for between-group differences with paired two-tailed t-test comparisons. Differences with P values < 0.05 were considered to be statistically significant.

Results

Memory impairment in a subpopulation of aged rats

We first investigated learning acquisition in young (5 months) and aged (>24 months) rats after water maze training consisting of 2 swims per day for 5 days. Aged rats were assigned to learning-unimpaired and learning-impaired groups based on the time it took to find a platform hidden under the surface of opaque water, reported as latency time, as described in Material and methods. There were significant differences among young, aged-unimpaired, and aged-impaired groups of animals in terms of learning acquisition during water maze training ($F_{2,128} = 57.960$, $P < 0.001$; Fig. 1A).

Ten days after the first 5-day swim, rats were trained for the second 5-day swim to induce memory retention. Twenty-four hours after the final training swim (see Material and methods), all animals underwent a probe test to evaluate whether they remembered the location of the platform despite being removed from the test area. Fig. 1B shows the differences in memory retention between the animal groups, quantified as the number of times the target area was crossed per minute. Significant differences in memory retention were observed between young, aged-unimpaired, and aged-impaired rats ($F_{5,56} = 4.089$; $P < 0.01$). In young rats, spatial memory training significantly increased memory retention compared with young rats that had not undergone training [*Young + maze training* vs. *Young* (*swim ctrl*); $P < 0.01$; Fig. 1B; Table 1]. Aged, learning-unimpaired rats did not exhibit memory impairment in the probe test compared with young rats ($F_{1,16} = 1.256$, $P = 0.28$; Fig. 1B; Table 1). By contrast, aged, learning-impaired rats showed significantly impaired memory retention compared with both aged-unimpaired ($F_{1,20} = 4.812$, $P < 0.05$) and young rats ($F_{1,15} = 8.873$, $P < 0.01$; Fig. 1B; Table 1).

Selective loss of mushroom spine synaptogenesis is associated with impaired memory in aged rats

Using electron microscopy of serial hippocampal sections and double-blind analysis at the level of single synapses (Figs. 2A and C), we found a significant difference among experimental groups in the number of all-shape dendritic spines ($F_{4,241} = 6.858$, $P < 0.001$; Fig. 2B) and mushroom spines ($F_{4,241} = 4.335$, $P < 0.05$; Fig. 2D). In young rats, spatial memory training increased the overall synaptic density ($P < 0.001$) and the density of mushroom spines ($P < 0.01$) in the CA1 stratum radiatum (CA3-to-CA1 pyramidal neuron connections) of the right dorsal hippocampus [Figs. 2B and D; compare *Young* with *Young* (*swim ctrl*); Table 1].

With spatial memory training, aged-impaired rats demonstrated a loss of total mushroom spine synaptogenesis (both macular and perforated PSDs), compared with young and aged-unimpaired rats ($P < 0.01$; Fig. 2D; Table 1), as well as a loss of mushroom spine synaptogenesis with only macular PSDs ($P < 0.01$; Fig. 2E; Table 1). The formation of mushroom spines with perforated PSDs was not impaired (Fig. 2F; Table 1), consistent with the observation that memory is not completely lost in aged-impaired rats (Fig. 1B). Thus, the loss of mushroom spine synaptogenesis in the apical dendrites of CA1 pyramidal neurons of aged-impaired rats correlated with the impaired memory retention observed in the probe test (Fig. 1B).

Bryostatin treatment restores synaptogenesis in aged rats with memory impairment

The age-related loss of synaptogenesis could be reversed with bryostatin treatment (5 μg/kg body wt., i.p., every other day for 10 days before and continued through water maze training), which increased mushroom spine synapses (both macular and perforated PSDs; $P < 0.01$, Fig. 2D, Table 1; and macular PSDs only, $P < 0.01$, Fig. 2E, Table 1) to the levels seen in young and aged-unimpaired animals (*dashed line*). In addition, bryostatin also restored memory decline in aged-impaired rats (Suppl. Fig. 1).

Electron microscopy also showed that in young rats, spatial memory training resulted in an increased concentration of presynaptic vesicles within axonal boutons that formed synapses with PSDs on mushroom spines (*Young* vs. *Young* (*swim ctrl*); $P < 0.05$; Figs. 2C and G; Table 1). Among rats that had undergone spatial memory training, the percentages of axonal boutons with a high concentration of presynaptic vesicles were not different with or without bryostatin (Figs. 2C and G; Table 1). This indicates that the increase in presynaptic vesicles was stimulated after water maze training in

Table 1
Summary statistics: changes in memory retention and the number/density of dendritic spines, synapses, and presynaptic membrane vesicles at the CA3-to-CA1 pyramidal neuron connection.

	Young rats swim control	Young rats + training	Aged, learning-unimpaired rats + training	Aged, learning-impaired rats + training	Aged, learning-impaired rats + training + bryostatin
Memory retention (probe test, times crossing target area per min; Fig. 1B)	0.33 ± 0.84*** n = 18 tests from 18 rats	1.70 ± 1.14 n = 12 tests from 12 rats	1.72 ± 1.19 n = 11 tests from 11 rats	0.80 ± 0.63** n = 10 tests from 10 rats	
Synapses per 5 × 5 μm² CA1 areas (EM):					
- All shape spine synapses (Fig. 2B)	10.5 ± 3.7***	14.0 ± 4.2	12.3 ± 3.5	9.7 ± 3.7	12.3 ± 5.0
- Mushroom-shaped spine synapses with					
• Macular + perforated PSDs (Fig. 2D)	0.5 ± 0.7**	1.0 ± 1.2	0.9 ± 1.4	0.4 ± 0.8**	1.0 ± 1.1++
• Macular PSDs (Fig. 2E)	0.4 ± 0.5**	0.7 ± 1.0	0.6 ± 1.0	0.2 ± 0.5**	0.7 ± 0.9++
• Perforated PSDs (Fig. 2F)	0.1 ± 0.3**	0.3 ± 0.5	0.3 ± 0.7	0.2 ± 0.5	0.3 ± 0.5
Concentration of presynaptic vesicles (EM; Fig. 2G)	29 ± 67%* n = 56 serial-section sets from 4 rats 1 (13–15 sets/rat)	54 ± 57% n = 50 serial-section sets from 3 rats (16–18 sets/rat)	52 ± 55% n = 45 serial-section sets from 3 rats (15 sets/rat)	51 ± 83% n = 41 serial-section sets from 4 rats (10–11 sets/rat)	54 ± 64% n = 64 serial-section sets from 4 rats (15–19 sets/rat)
Spines/100 μm dendritic shaft (DiI staining):					
- All-shape spines (Fig. 3B)	250.4 ± 25.5*	296.0 ± 49.0	301.1 ± 51.3	230.0 ± 41.4*	298.0 ± 51.2+
- Mushroom-shaped spines (Fig. 3C)	30.8 ± 24.2** n = 34 dendrites (≈24 neurons) from 4 rats (5–7 neurons/rat)	59.3 ± 39.2 n = 28 dendrites (≈22 neurons) from 4 rats (4–6 neurons/rat)	57.7 ± 24.1 n = 36 dendrites (≈22 neurons) from 4 rats (4–6 neurons/rat)	32.2 ± 32.6** n = 23 dendrites (≈18 neurons) from 4 rats (4–5 neurons/rat)	58.8 ± 21.4++ n = 35 dendrites (≈25 neurons) from 4 rats (5–7 neurons/rat)
All-shape spines per 63 × 63 μm² (immunocytochemistry; Fig. 3E)	82 ± 13%** n = 40 areas from 4 rats (10 areas/rat)	100 ± 21% n = 28 areas from 4 rats (7 areas/rat)	89 ± 25% n = 35 areas from 4 rats (8–9 areas/rat)	83 ± 17%** n = 36 areas from 4 rats (9 areas/rat)	97 ± 11%** n = 26 areas from 4 rats (5–6 areas/rat)
CA1 pyramidal neuron cell bodies per 40 × 40 μm² (Fig. 3F)		11.0 ± 1.8 n = 48 areas from 4 rats (12 areas/rat)	10.5 ± 1.6 n = 48 areas from 4 rats (12 areas/rat)	10.5 ± 1.7 n = 48 areas from 4 rats (12 areas/rat)	10.4 ± 1.4 n = 48 areas from 4 rats (12 areas/rat)

Data are reported as mean ± SD; n = number of measurements used for SD calculation and statistical analysis, ANOVA for memory retention (probe test) and two-tailed paired t-test for dendritic spines and synapses. For probe test, one probe test swim per rat. For dendritic spines and synapses, multiple measurements were collected from 4 hippocampal sections (approximately 600 μm apart along dorsal hippocampus) per rat. For DiI staining, the DiI-coated tip of the micropipette glass stained several neurons; and each DiI-stained area was completely isolated from other DiI-stained areas. One (and sometimes two or three) dendritic shaft was analyzed from each DiI-stained CA1 area. The number of CA1 pyramidal neurons used for DiI staining as shown in the table was the minimum number (one neuron in each CA1 area) and the maximum number of neurons was no more than the number of dendritic shafts (if each dendritic shaft came from one neuron). EM = electron microscopy; PSDs = postsynaptic densities.

* $P < 0.05$ compared with young rats + water maze training.
** $P < 0.01$ compared with young rats + water maze training.
*** $P < 0.001$ compared with young rats + water maze training.
\+ $P < 0.05$ comparison of aged, learning-unimpaired rats with and without bryostatin treatment, or comparison of aged, learning-impaired rats with and without bryostatin treatment.
++ $P < 0.01$ comparison of aged, learning-unimpaired rats with and without bryostatin treatment, or comparison of aged, learning-impaired rats with and without bryostatin treatment.

Table 2
Summary statistics: changes in molecular measures (PKC/HuD/BDNF cascade) and electrophysiology underlying synaptic formation and maintenance.

	Young rats + training	Aged, learning-impaired rats + training	Aged, learning-impaired rats + training + bryostatin
PKC level in the whole right hippocampus:			
- PKCε immunoblot (Fig. 4B)	100 ± 29%	74 ± 9%*	105 ± 14%$^{+}$
- PKCα immunoblot (Fig. 4C)	100 ± 20%	69 ± 10%*	108 ± 6%$^{+}$
	n = 5 right hippocampi from 5 rats	n = 3 right hippocampi	n = 4 right hippocampi
PKCε level in the mossy fibers (dentate gyrus-to-CA3 in right dorsal hippocampus; immunohistochemistry and confocal microscopy; Fig. 5B)	100 ± 25%	89 ± 25%*	112 ± 45%$^{+}$
	n = 40 areas from 4 rats (10 areas/rat)	n = 40 areas from 4 rats (10 areas/rat)	n = 40 areas from 4 rats (10 areas/rat)
No. PKCε-containing axonal boutons of the Schaffer collateral fibers (CA3-to-CA1in right dorsal hippocampus; immunohistochemistry and confocal microscopy; Fig. 5D)	100 ± 27%	85 ± 38%*	101 ± 39%$^{+}$
	n = 60 CA1 area from 6 rats (10 areas/rat)	n = 40 CA1 area from 4 rats (10 areas/rat)	n = 40 CA1 area from 4 rats (10 areas/rat)
PKCα level in CA1 pyramidal neurons (in right dorsal hippocampus; immunohistochemistry and confocal microscopy; Fig. 5I)	100 ± 22%	80 ± 18%***	103 ± 34%$^{+++}$
	n = 272 neurons from 4 rats (16 areas/rat)	n = 184 neurons from 4 rats (12 areas/rat)	n = 207 neurons from 3 rats (12 areas/rat)
PKC-activated nuclear export and activation of the mRNA-stabilizing protein HuD (in right dorsal hippocampus; immunohistochemistry and confocal microscopy; Fig. 6B)	100 ± 24%	84 ± 32%***	97 ± 35%$^{+++}$
	n = 148 neurons from 4 rats (8 areas/rat)	n = 137 neurons from 4 rats (8 areas/rat)	n = 132 neurons from 4 rats (8 areas/rat)
BDNF expression in CA1 pyramidal neuron cell bodies (in right dorsal hippocampus; immunohistochemistry and confocal microscopy; Fig. 6D)	100 ± 21%	84 ± 25%***	100 ± 28%$^{+++}$
	n = 135 neurons from 4 rats (8 areas/rat)	n = 171 neurons from 4 rats (8 areas/rat)	n = 123 neurons from 3 rats (8 areas/rat)
BDNF expression in CA1 pyramidal neuron distal dendrites (in right dorsal hippocampus; immunohistochemistry and confocal microscopy; Fig. 6E)	100 ± 17%	83 ± 15%***	108 ± 24%$^{+++}$
	n = 40 CA1 area from 4 rats (10 areas/rat)	n = 40 CA1 area from 4 rats (10 areas/rat)	n = 40 CA1 area from 4 rats (10 areas/rat)
GABAergic synaptic transmission in the CA1 pyramidal neurons (electrophysiology) fh:			
- Synaptic transmission (Hz) (Fig. 7B)	2.37 ± 0.82	6.06 ± 3.75**	3.18 ± 1.11^{++}
- sIPSC (pA) (Fig. 7C)	61.23 ± 32.92	92.99 ± 46.33*	64.02 ± 23.87^{++}
	n = 10 neurons	n = 13 neurons	n = 12 neurons

Data are reported as mean ± SD; n = number of measurements used for SD calculation and statistical analysis [1 measurement per rat for immunoblots; multiple measurements from 4 hippocampal sections (approximately 600 μm apart along dorsal hippocampus) per rat for immunohistochemistry of PKC, HuD, and BDNF; and 1–2 neurons per rat for electrophysiology].

* $P < 0.05$ paired t-test, compared with young rats.
** $P < 0.01$ paired t-test, compared with young rats.
*** $P < 0.001$ paired t-test, compared with young rats.
$^{+}$ $P < 0.05$ paired t-test, compared with aged, learning-impaired rats without bryostatin treatment.
$^{++}$ $P < 0.01$ paired t-test, compared with aged, learning-impaired rats without bryostatin treatment.
$^{+++}$ $P < 0.001$ paired t-test, compared with aged, learning-impaired rats without bryostatin treatment.

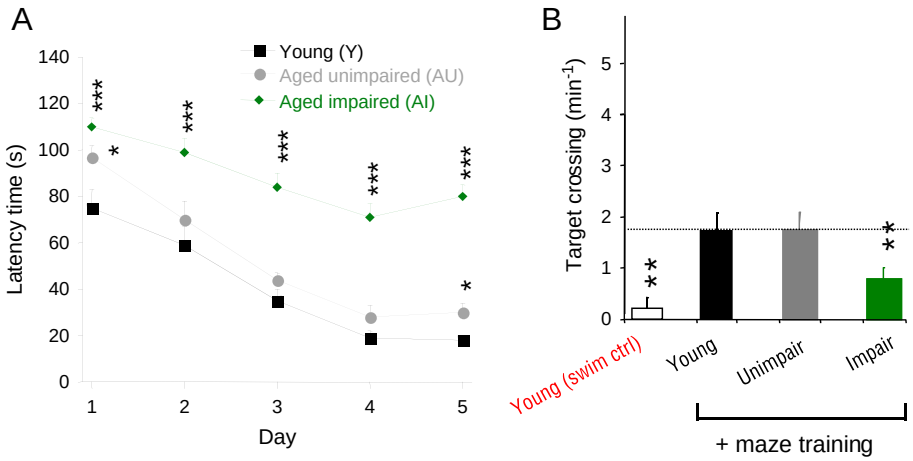

Fig. 1. Spatial memory decline in a subpopulation of aged rats. (A) Learning curves during the first water maze training (2 swims per day), showing latency time, defined as the time taken for rats to reach a hidden underwater platform. Latency time was used to divide aged rats into learning-unimpaired and learning-impaired groups compared to young controls. (B) Ten days after the first 5-day water maze training, rats underwent a second 5-day water maze training (2 swims per day). Memory retention was determined by a probe test conducted 24 h after the last swim of the second 5-day water maze training. Data are presented as mean ± SEM; $^{*}P < 0.05$, $^{**}P < 0.01$, $^{***}P < 0.001$; ANOVA. Asterisks, compared with young + maze. *Swim ctrl* = swim control; unimpair = aged, learning-unimpaired; impair = aged, learning-impaired.

aged rats, even in those animals that demonstrated memory impairment in the probe test.

Selective loss of mushroom spine formation is associated with impaired memory in aged rats

Using DiI staining and confocal microscopy with 3D deconvolution and double-blind analysis, we determined the dendritic spine density on individual apical dendrites of CA1 pyramidal neurons in the hippocampal CA1 stratum radiatum in young and aged rats after water maze training (Fig. 3A). We found a significant difference among experimental groups in the number of all-shape dendritic spines ($F_{2,85} = 3.307$, $P < 0.05$) and mushroom spines ($F_{4,153} = 4.746$, $P < 0.01$). In young rats, spatial memory training increased the overall spine density and the density of mushroom spines (CA3-to-CA1 pyramidal neuron connections per 100 μm dendritic shaft) in the CA1 stratum radiatum of the right dorsal hippocampus [Figs. 3B and C; compare *Young* with *Young* (*swim ctrl*); Table 1]. Both total dendritic spine density and mushroom spine density ($P < 0.01$) of aged-impaired rats were significantly lower compared with young and aged-unimpaired rats (Figs. 3B and C; Table 1).

We further assessed the density of all dendritic spines in the hippocampal CA1 stratum radiatum using an antibody against the dendritic spine-specific protein spinophilin (Fig. 3D). A significant difference among experimental groups was found ($F_{5,189} = 6.114$, $P < 0.001$). As shown in Fig. 3E and Table 1, dendritic spine density after water maze training was lower in aged-impaired animals compared with young and aged-unimpaired controls ($P < 0.01$). As one dendritic spine can form more than one synapse, these results suggest that the loss of synaptogenesis in aged rats is the consequence of a defect of dendritic spine generation rather than the loss of multiple synapses on a constant number of dendritic spines.

Bryostatin restores total and mushroom spine formation after spatial memory training in the CA1 stratum radiatum of aged rats

In aged-impaired rats, bryostatin significantly increased total dendritic spine density, as seen with DiI staining ($P < 0.01$; Fig. 3B; Table 1) and with spinophilin immunohistochemistry ($P < 0.01$; Fig. 3E; Table 1), to levels comparable to those seen in young and aged-unimpaired rats (*dashed lines*). Bryostatin treatment also increased mushroom spine density in aged-impaired rats, again to levels comparable to those seen in young and aged-unimpaired rats ($P < 0.01$; Fig. 3C, *dashed line*; Table 1). Thus, bryostatin treatment combined with spatial memory training restored memory-activated mushroom spinogenesis on dendrites in aged-impaired rats. These data suggest that the bryostatin-induced restoration of synaptogenesis in aged rats is a consequence of the rescue of dendritic spinogenesis, and not the generation of multiple synapses on the existing dendritic spines.

Lower dendritic spine density in aged rats after training is not due to increased neuronal/brain volume

The hippocampal CA1 stratum radiatum of aged rats is susceptible to increases in volume after histologic preparation, resulting in an apparent decrease in neuronal cell number per unit brain volume compared with adult rats (Geinisman et al., 2004). This observation may be related to a reduction of proteins responsible for the degradation of reactive oxygen species in aged brain cells. Because prolonged perfusion fixation through the heart can induce ultrastructural tissue changes (Tao-Cheng et al., 2007), we shortened the PBS perfusion time to <4 min for confocal microscopy and 5 s for electron microscopy prior to aldehyde fixation to reduce neuronal degeneration/swelling stimulated by hypoxia and oxidative stress.

Using morphometrics and ANOVA, we confirmed that there were no significant differences among animals in each experimental group in terms of pyramidal neuronal cell density ($F_{4,239} = 0.994$, $P > 0.5$; Fig. 3F; Table 1) or cell volume (*not shown*) in the CA1 stratum pyramidale of the dorsal hippocampus. Thus, our modified perfusion fixation procedure resulted in no decrease in CA1 pyramidal neuron density or enlargement of CA1 pyramidal neurons in the dorsal hippocampus, and we are confident that the observed lower number of mushroom and all spine densities on dendritic shafts in aged rats are not due to an increase in the volume of CA1 stratum radiatum or neuronal cell death. Furthermore, increased dendritic spinogenesis at the level of a single dendritic shaft/neuron (Figs. 3A–C) with no increase in the number of neurons (Fig. 3F) suggests that bryostatin-induced restoration of mushroom dendritic spinogenesis occurs in the existing neurons rather than via neurogenesis.

The PKCε-specific activator DPC-LA restores dendritic spinogenesis in aged-impaired rats

To investigate whether activation of PKCε, independent of PKCα, could restore spinogenesis in aged-impaired rats, we treated rats with

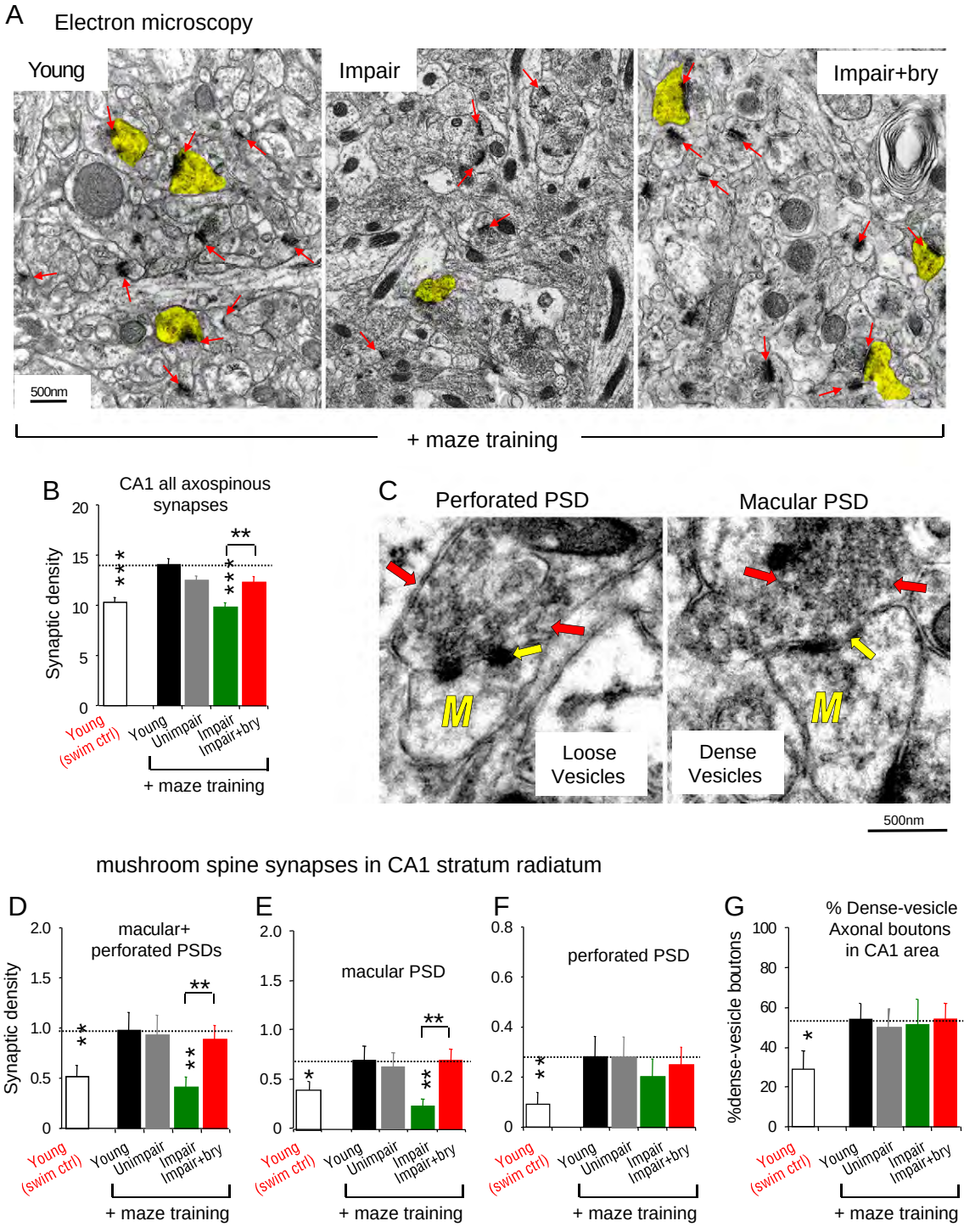

Fig. 2. Bryostatin treatment during spatial memory training restores mushroom dendritic spine synaptogenesis in aged rats. Data were collected using right dorsal hippocampal tissue collected 24 h after memory retention was evaluated. (A) Electron microscopy of the stratum radiatum in the right dorsal hippocampal CA1 area. Mushroom spine synapses are highlighted in yellow; red arrows point to all axospinous synapses of mushroom, thin, and stubby dendritic spines. (B) All axospinous synapses per $5 \times 5 \times 0.09$ μm^3 of serial CA1 stratum radiatum sections increased in young rats after memory retention (Young) compared with young rats without memory retention [Young (swim control)]. After spatial memory training (dashed line), bryostatin treatment combined with water maze training restored synapse density in aged-impaired rats to the levels seen in young rats (*dashed line*). (C) Electron micrographs show that mushroom dendritic spines (M) form synapses (red arrows) with axonal boutons containing presynaptic vesicles (white arrows). Synapses had macular (continuous) or perforated (discontinuous) postsynaptic densities (PSDs). Density of (D) mushroom spine synapses with both macular and perforated PSDs, (E) mushroom spine synapses with macular PSDs only, (F) mushroom spine synapses with perforated PSDs only, and (G) axonal boutons with a high concentration of presynaptic vesicles. Data are presented as mean ± SEM; $^{*}P < 0.05$, $^{**}P < 0.01$, $^{***}P < 0.001$; paired t-test. Asterisks over bars, compared with young; asterisks over brackets, comparison of untreated and treated animals in each group. *Swim ctrl* = swim control; impair = aged, learning-impaired; bry = bryostatin.

the PKCε-specific activator DCP-LA (Hongpaisan et al., 2011; Nelson et al., 2009) combined with spatial memory training. As measured by DiI staining, significant differences were found among experimental groups for the overall spine density ($F_{2,164} = 5.341$, $P < 0.01$; Fig. 3G) and the density of mushroom spines ($F_{2,164} = 3.570$, $P < 0.05$; Fig. 3H). In aged-impaired rats, the loss of overall and mushroom dendritic spines [mean ± SD spines/100 μm dendritic shaft: 229 ± 99 overall spines and 29 ± 12 mushroom spines (n = 38 shafts from 4

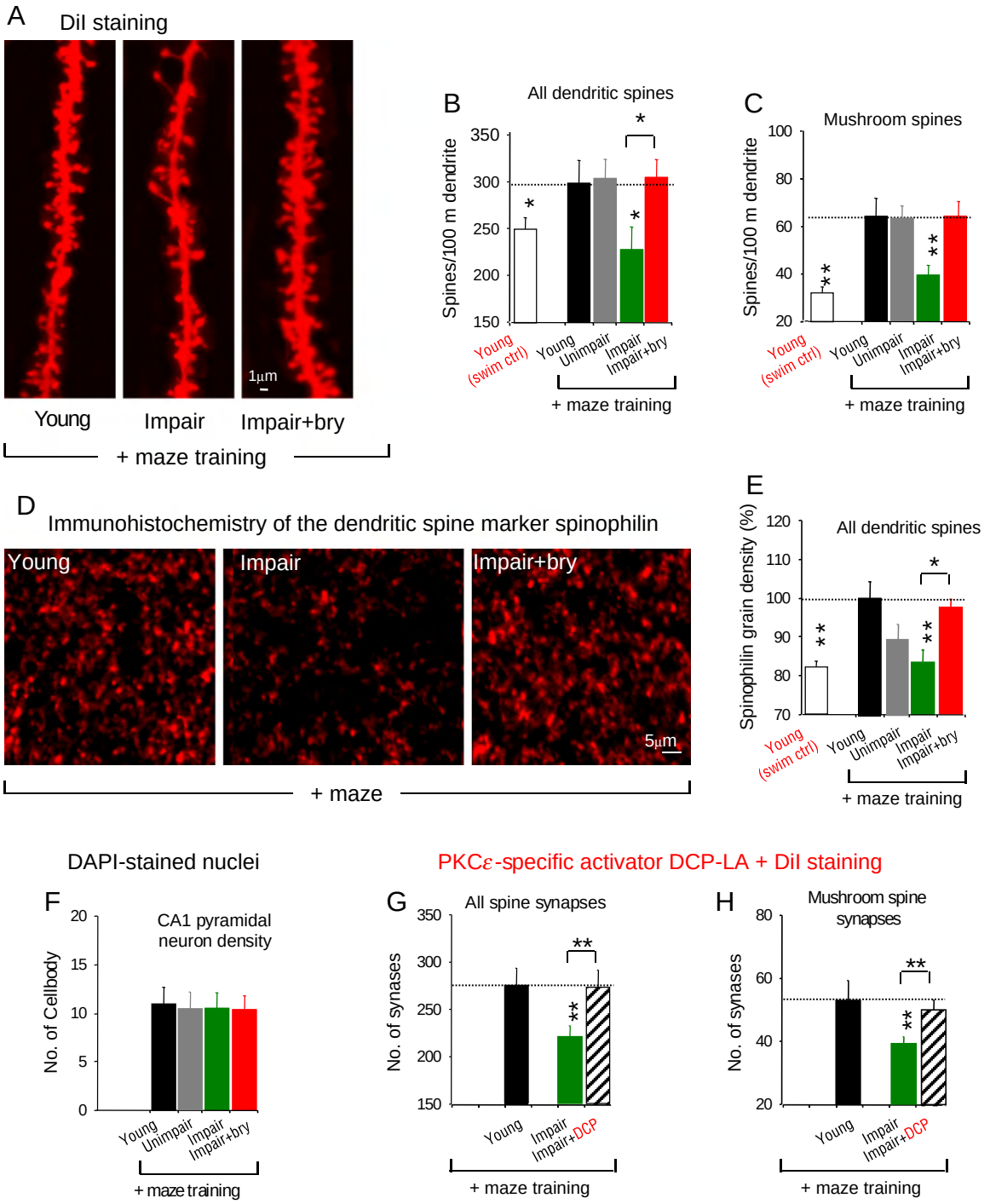

Fig. 3. Bryostatin restores the formation of mushroom dendritic spines in the CA1 pyramidal neurons of aged, learning-impaired rats. Analysis was performed in right dorsal hippocampal tissues collected 24 h after memory retention was evaluated in the probe test. (A) Confocal microscopy at the single dendritic spine level was analyzed with serial scanning, 3-D reconstruction, and double-blind quantification. The number of (B) all (mushroom, thin, and stubby) and (C) mushroom-dendritic spines per 100 μm of individual apical dendrites increased in young rats after memory retention in a probe test (Young) compared with young rats without memory training [Young (swim control)]. After spatial memory training (*dashed line*), aged-impaired rats had a lower capacity to generate dendritic spines compared with young rats, which was reversed with bryostatin. (D, E) Confocal microscopy and immunohistochemistry of the dendritic spine-specific protein spinophilin confirmed the decreased dendritic spine density per 63 × 63 × 0.6 μm^3 of CA1 stratum radiatum in aged rats, which could be reversed by bryostatin. (F) The density of CA1 pyramidal neuron nuclei stained with DAPI indicated that there was no difference in the number and volume of CA1 pyramidal neurons in the experimental groups due to histologic tissue preparation. (G) Treatment with the PKCε-specific activator DCP-LA (1.5 mg/kg, i.p.), using the same regimen as for bryostatin in Fig. 2A, was sufficient to restore the decrease in dendritic spine density, using DiI staining, in aged-impaired rats. Data are presented as mean ± SEM; $^{*}P < 0.05$, $^{**}P < 0.01$; paired t-test. Asterisks over bars, compared with young; asterisks over brackets, comparison of untreated and treated animals in each group. *Swim ctrl* = swim control; impair = aged, learning-impaired; bry = bryostatin; DCP = DCP-LA.

aged-impaired rats) compared to 285 ± 117 overall spines and 46 ± 31 mushroom spines (n = 67 shafts from 4 young rats); $P < 0.01$] was restored ($P < 0.01$) after treatment with DCP-LA [284 ± 138 overall spines and 40 ± 20 mushroom spines (n = 60 shafts from 4 aged impaired rats treated with DCP-LA)] (Figs. 3G and H).

Reduced PKCε/α in the aged rat hippocampus correlates with impaired learning and memory retention

Next, we investigated the molecular mechanisms underlying the observed changes at the level of the dendritic spine and synapse. We first

evaluated PKCε and PKCα levels in the whole right hippocampus by immunoblot, with the researcher performing the quantification and analysis blinded to the treatment group of each hippocampal lysate. A significant difference between experimental groups was seen in hippocampal expression of PKCε ($F_{4,19} = 3.291$, $P < 0.05$) and PKCα ($F_{4,19} = 5.735$, $P < 0.01$). Aged-impaired rats had significantly lower PKCε and PKCα levels compared with young animals ($P < 0.05$; Fig. 4; Table 2).

PKCε levels in the right dorsal hippocampal circuitry were also assessed by immunohistochemistry and confocal microscopy (Fig. 5A). There was a significant difference among experimental groups in PKCε expression in the mossy fibers, which are composed of axons of granule cells in the dentate gyrus that synapse with dendritic spines of CA3 pyramidal neurons ($F_{4,199} = 4.241$, $P < 0.01$; Fig. 5B). Compared with young rats, the PKCε content in the mossy fibers was reduced in aged-impaired rats ($P < 0.05$; Fig. 5B; Table 2).

The densities of PKCε-containing axonal boutons of the Schaffer collateral fibers in the hippocampal CA1 stratum radiatum were further examined with double immunohistochemistry of PKCε and the presynaptic vesicle membrane protein synaptophysin (Fig. 5C). At the resolution limit of confocal microscopy, 1 synaptophysin-positive grain represented 1 axonal bouton, and fluorescence intensity of synaptophysin-positive grains indicated the concentration of presynaptic vesicle membranes. Confocal images were taken at 0.6-μm thickness to ensure that each counted grain represented only 1 axonal bouton, and not an overlay of more than 2 boutons. ANOVA showed a significant difference in PKCε-containing axonal boutons among aged-impaired rat and young control groups ($F_{2,126} = 2.953$, $P < 0.05$; Fig. 5D; Table 2). Paired t-testing also revealed a significant difference in the density of PKCε-containing axonal boutons in aged-impaired rats ($P < 0.05$), compared with young controls (Fig. 5D). There was no significant difference in the Manders overlap coefficient for colocalization of PKCε and axonal boutons, even after adjustment of signal intensities between the 2 channels, photo-bleaching, and changing the amplifier setting (Fig. 5E). There was also no difference in the overall density of axonal boutons (with or without PKCε; Fig. 5F) or in the density of presynaptic vesicles within the axonal boutons (Fig. 5G), confirming the results studied with electron microscopy (Fig. 2F). These findings suggest that the lower density of PKCε-containing boutons in aged-impaired rats is due to the loss of PKCε expression within the axonal boutons, and not a loss of axonal boutons.

Finally, we assessed PKCα expression at the level of single CA1 pyramidal neuron cell bodies in the right dorsal hippocampus by immunohistochemistry and confocal microscopy (Fig. 5H). Significant differences were seen between the experimental groups ($F_{5,1157} = 39.030$, $P < 0.001$). Compared with young rats, there were significantly lower levels of PKCα expression in the hippocampal CA1 pyramidal neurons of aged-impaired rats ($P < 0.001$; Fig. 5I; Table 2). Together, these results indicate that a selective loss of PKCε-containing presynaptic boutons and a reduction of postsynaptic PKCα in CA1 pyramidal neurons are associated with age-related impaired learning and memory retention in rats.

Bryostatin restores PKCε and PKCα expression in the aged rat hippocampal circuit

At the level of the whole right hippocampus, bryostatin restored expression of both PKCε and PKCα isozymes to the levels seen in young animals ($P < 0.05$; Fig. 4, *dashed line*; Table 2). At the cellular

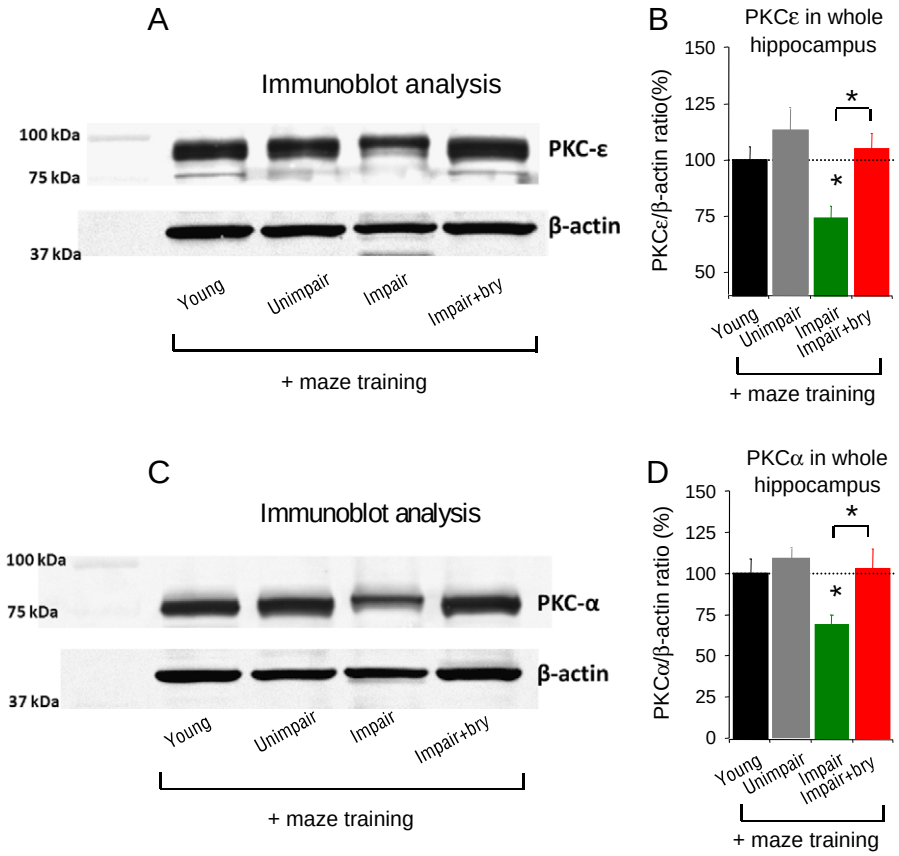

Fig. 4. Bryostatin restores PKCε and α levels in the right hippocampus in aged, learning-impaired rats. Immunoblot analysis of whole hippocampal lysates from aged-impaired rats collected 24 h after memory retention was evaluated by probe test, showed decreased levels of (A, B) PKCε and (C, D) PKCα that were restored by bryostatin treatment. Data are presented as mean ± SEM; *$P < 0.05$, paired t-test. Asterisks over bars, compared with young; asterisks over brackets, comparison of untreated and treated animals in each group. Impair = aged, learning-impaired; bry = bryostatin.

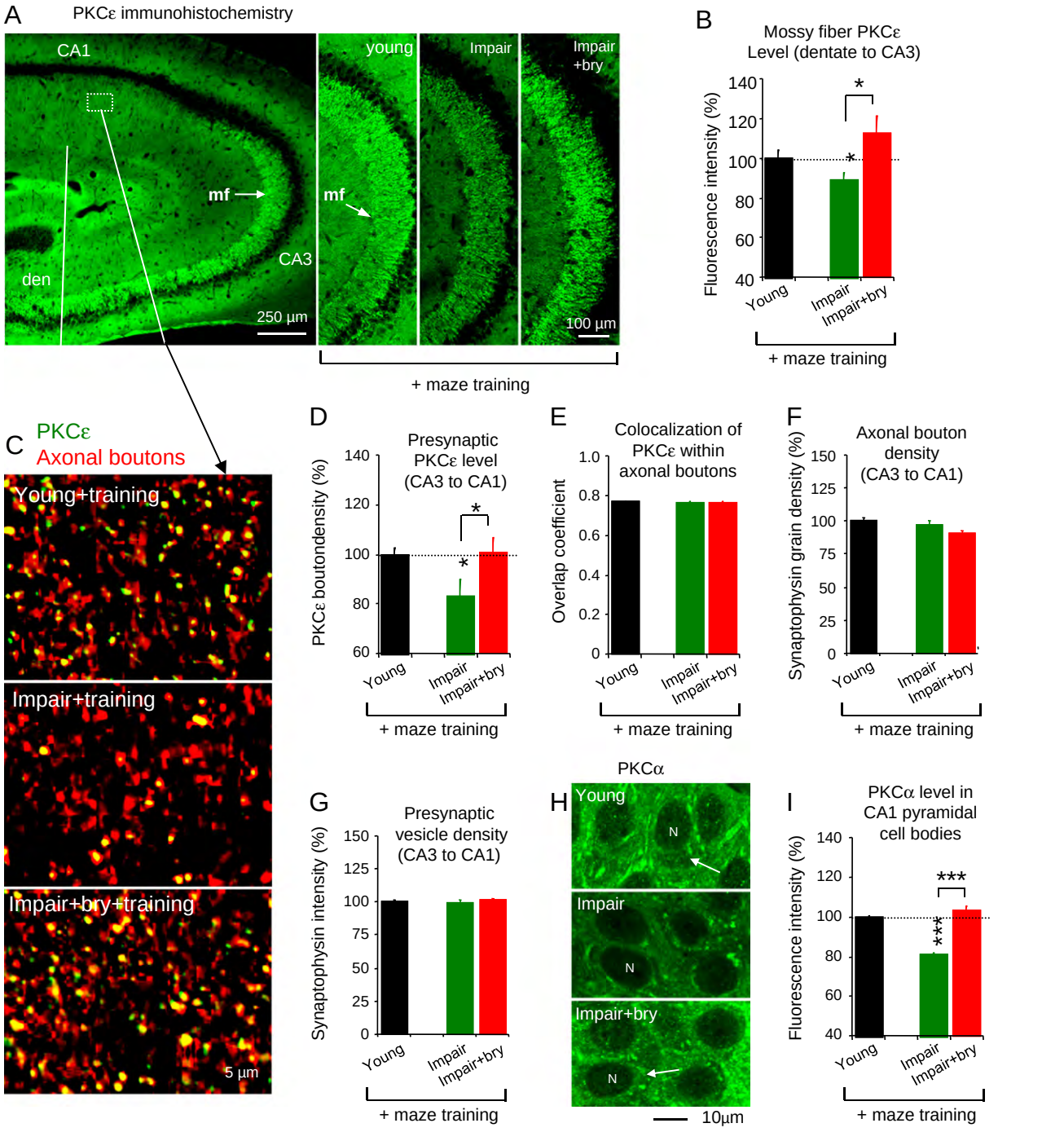

Fig. 5. Bryostatin restores PKCε and PKCα levels in the hippocampal circuitry of aged rats. Measurement was conducted in right dorsal hippocampal tissues collected 24 h after memory retention was evaluated. (A, B) Confocal immunohistochemistry revealed that in aged rats, bryostatin restored PKCε levels in the mossy fibers (mf), the granule cell axons from the dentate gyrus (den) to CA3 pyramidal neurons. (C) Double immunostaining of PKCε (green) and axonal boutons (synaptophysin; red) of the Schaffer collateral fibers, which are axons of CA3 pyramidal neurons that synapse with apical dendrites of CA1 pyramidal neurons (in the CA1 stratum radiatum). (D) The density of PKCε-containing axonal boutons [yellow overlay in (C)] in the CA1 stratum radiatum was reduced in aged-impaired rats and restored by bryostatin. (E) The overlap coefficient showed that the reduced PKCε in axonal boutons at the CA3–CA1 connection in aged-impaired rats was not a result of PKCε dislocation. The densities of (F) all axonal boutons (with and without PKCε) and (G) their presynaptic vesicles were not different between experimental groups. (H) Confocal immunocytochemistry showed that (I) decreased PKCα within the cell bodies of CA1 pyramidal neurons in aged rats could be rescued by bryostatin. Data are presented as mean ± SEM; $^{*}P < 0.05$, $^{***}P < 0.00$; paired t-test. Asterisks over bars, compared with young; asterisks over brackets, comparison of untreated and treated animals in each group. Impair = aged, learning-impaired; bry = bryostatin.

level, bryostatin treatment restored PKCε expression in the mossy fibers in aged-impaired rats to the levels observed in young rats ($P < 0.05$; Fig. 5B, *dashed line*; Table 2). PKCε-containing axonal boutons in aged-impaired rats were also restored by bryostatin treatment ($P < 0.05$; Fig. 5D, *dashed line*; Table 2), as were PKCα levels in the cell bodies of CA1 pyramidal neurons ($P < 0.001$; Fig. 5I, *dashed line*; Table 2). These data suggest that activation of PKCε and PKCα by bryostatin induces expression of these PKC isozymes in the hippocampal circuitry.

Aging affects HuD and BDNF, downstream molecular targets for PKC

Because we observed an age-dependent decrease in PKCε and PKCα expression in the hippocampus, we investigated whether the localization

and activity of HuD – a substrate of both PKCε and PKCα involved in post-transcriptional mRNA stability (Pascale et al., 2005) – and PKCε- and PKCα-dependent BDNF expression (Sun et al., 2008) were also affected in the right dorsal hippocampal circuitry of aged, learning-impaired rats. Using immunohistochemistry and confocal microscopy, we observed significant differences among experimental groups in the cytoplasmic/nuclear ratio of HuD (Figs. 6A and B; $F_{4,717} = 6.726$, $P < 0.001$); in BDNF expression in cell bodies of pyramidal neurons in the right dorsal hippocampal CA1 area (Figs. 6C and D; $F_{4,755} = 18.614$, $P < 0.001$); and in BDNF expression in the CA1 stratum radiatum (Figs. 6C and E; $F_{4,196} = 11.005$, $P < 0.001$). Compared with young rats, aged-impaired rats showed impaired nuclear export (i.e., activation) of HuD ($P < 0.001$; Fig. 6B; Table 2) and lower levels of BDNF protein in CA1 pyramidal neurons ($P < 0.001$; Fig. 6D; Table 2). Notably, this decrease in HuD activation and BDNF expression correlated with lower PKCα expression observed in the perinuclear cytoplasm of CA1 pyramidal neurons (Fig. 5I). Furthermore, compared with young animals, BDNF expression was significantly reduced in the CA1 stratum radiatum of aged-impaired rats ($P < 0.001$; Fig. 6E; Table 2), which also paralleled the selective reduction of PKCε-containing axonal boutons in the CA1 stratum radiatum observed in aged-impaired rats (Fig. 5D). These results suggest that the loss of HuD and BDNF in aged rats occurred as a consequence of a loss of PKCε/α expression in the aging right dorsal hippocampal circuitry.

Bryostatin restores HuD-dependent mRNA stabilization and BDNF expression in aged rats

Bryostatin treatment restored the nuclear export and activation of HuD in aged-impaired rats to the levels seen in young rats ($P < 0.001$; Fig. 6B, *dashed line*). Bryostatin treatment also restored levels of BDNF expression in CA1 pyramidal neurons in aged-impaired rats to levels seen in young rats ($P < 0.001$; Fig. 5D, *dashed line*; Table 2). Likewise, bryostatin treatment recovered the selective loss of BDNF in the CA1 stratum radiatum in aged-impaired rats to levels seen in young rats ($P < 0.001$; Fig. 5E, *dashed line*; Table 2). These results suggest that bryostatin-induced recovery of PKCε and PKCα levels restored the age-related loss of HuD activity and BDNF expression in the pyramidal neurons of rats.

Changes in GABAergic synaptic transmission in the CA1 pyramidal neurons

Previous studies suggest that normal aging disturbs the balance of excitatory and inhibitory transmission, and that aging leads to decreased synaptic excitation and increased synaptic inhibition in the prefrontal cortex and hippocampus (Luebke et al., 2004; Peters et al., 2008; Xu et al., 2009). We studied changes in synaptic transmission in the CA1 pyramidal neurons and their correlation with age-associated cognitive dysfunction. Spontaneous inhibitory postsynaptic currents (sIPSC) in

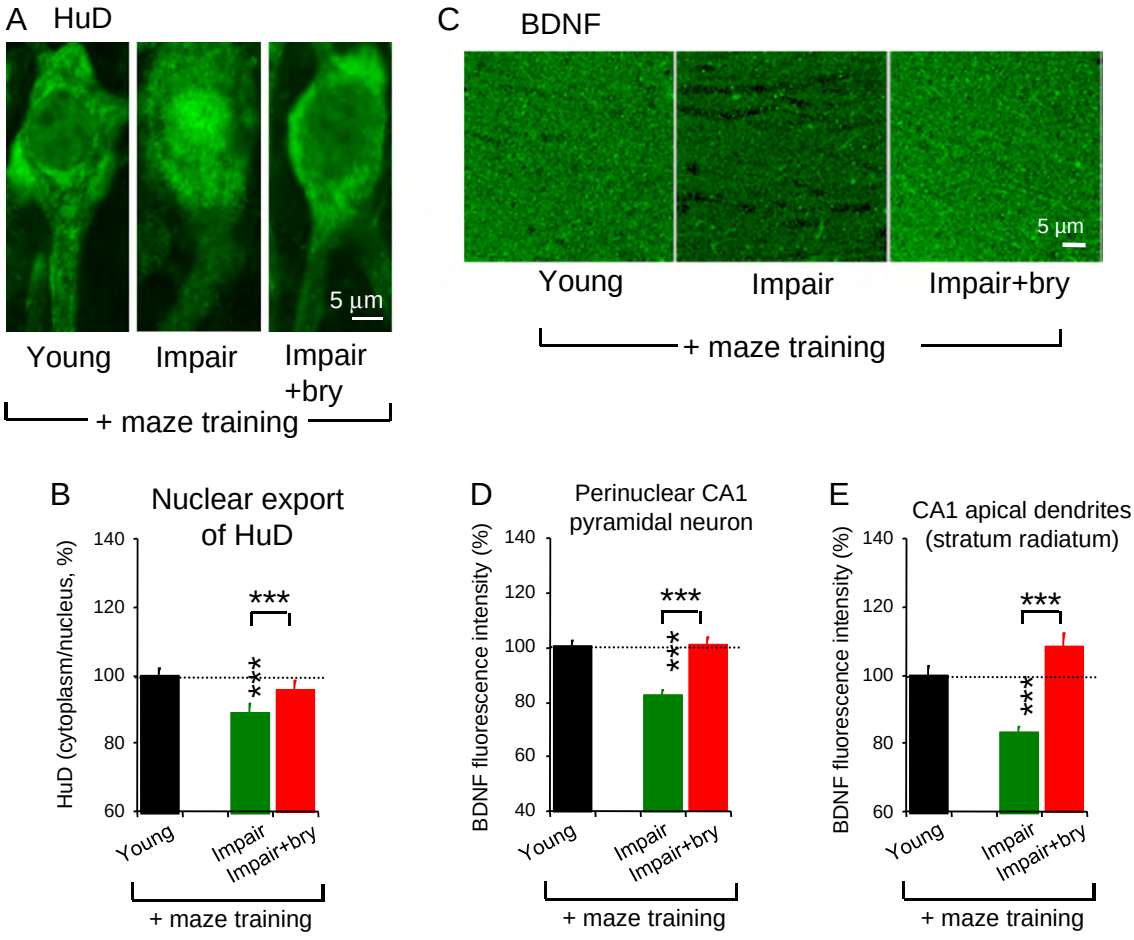

Fig. 6. Bryostatin restores PKC-activated HuD activity and BDNF expression in CA1 pyramidal neurons of aged rats. Measurement was obtained from right dorsal hippocampal tissues collected at 24 h after memory retention was evaluated in the probe test (Fig. 2A). (A) Confocal microscopy and immunohistochemistry of the mRNA-stabilizing protein HuD. (B) Nuclear export and activation of HuD and subsequent transport into dendrites were reduced in aged rats and were reversed with bryostatin. (C) Confocal immunohistochemistry of the HuD target BDNF in the CA1 stratum radiatum. In aged-impaired rats compared with young rats, BDNF levels were reduced and restored by bryostatin in both (D) the perinuclear cell bodies and (E) dendrites of CA1 pyramidal neurons. Data are presented as mean ± SEM; $^{**}P < .01$; $^{***}P < .001$; paired t-test. Asterisks over bars, compared with young; asterisks over brackets, comparison of untreated and treated animals in each group. Impair = aged, learning-impaired; bry = bryostatin.

the CA1 pyramidal neurons were measured with whole-cell patch-clamp recording (Fig. 7A). We found that young rats and aged-unimpaired rats have similarly low frequency and amplitude sIPSCs (data not shown), whereas aged-impaired rats have higher frequency ($P < 0.01$) and amplitude ($P < 0.05$) sIPSCs (Figs. 7B and C; Table 2). A paired-pulse stimulation protocol was used to evaluate short-term GABAergic synaptic plasticity in aged-unimpaired (n = 9 neurons) and aged-impaired rats (n = 13 neurons) in the presence of AP5 and DNQX (Fig. 8D). We found that short-term GABAergic synaptic plasticity was not changed (Fig. 7D); however, GABAergic long-term depression (I-LTD) was induced in the aged-unimpaired group (90%, 9 out of 10 cells from 8 rats), but not in the aged-impaired group (14 cells from 8 rats), which suggested that long-term GABAergic synaptic activity was different between the two groups of aged animals (Fig. 7E). Compared with untreated controls, aged-impaired rats treated with bryostatin showed a decrease in the frequency and amplitude of sIPSC ($P < 0.01$), returning them to levels similar to those seen in young control rats (Figs. 7B and C; Table 1).

Bryostatin, without water maze training, increases non-mushroom dendritic spine density and synaptic membrane density in aged rats

We previously observed in young rats (4–5 months) that bryostatin treatment increased non-mushroom dendritic spine and presynaptic membrane densities (Hongpaisan and Alkon, 2007). Based on these observations, we verified whether this effect of bryostatin also occurred in aged rats (>24 months). Dendritic spines on individual apical dendritic shafts of CA1 pyramidal neurons (stratum radiatum) were stained with DiI and imaged with confocal microscopy by serial scanning, 3D reconstruction analysis, and a double-blind analysis (Fig. 8A). Bryostatin treatment increased the density of all dendritic spines in aged rats [164 ± 33 (mean ± SD) spines/100 μm dendritic shaft, n = 22 dendrites from 3 rats, 4 hippocampal sections per rat; Figs. 8A and B] compared with those of untreated aged rats (131 ± 48 spines in n = 23 dendrites from 3 rats, 4 hippocampal sections per rat; $P < 0.001$). However, bryostatin did not significantly increase the density of mushroom dendritic spines in aged rats (Fig. 8C), suggesting that bryostatin increased the number of non-mushroom spines.

Using immunohistochemistry and confocal microscopy (Figs. 8D,G), changes in the densities of pre- and postsynaptic structures were studied in the CA1 stratum radiatum of aged rats. Compared with untreated controls, bryostatin treatment increased the densities of postsynaptic dendritic spines (spinophilin grains, from 100 ± 44% to 166 ± 24%; $P < 0.001$; Fig. 8E), but not axonal boutons [synaptophysin grains, from 100 ± 52% to 100 ± 51%; $P = 0.59$; Fig. 8F; n = 19 − 25 CA1 stratum radiatum areas (63 × 63 μm^2) from 3 rats and 4 hippocampal sections per rat in each experimental group]. Compared with untreated controls, bryostatin treatment increased the densities of postsynaptic membranes (neurogranin grains, from 100 ± 60% to 154 ± 88%; $P < 0.05$; Fig. 8H) and presynaptic membranes [GAP-43 grains, from 100 ± 27% to 125 ± 27%; $P < 0.001$; Fig. 8I; n = 30 CA1 stratum radiatum areas (63 × 63 μm^2) from 3 rats and 4 hippocampal sections per rat in each experimental group].

Taken together, although bryostatin treatment increased the density of total dendritic spines and pre- and postsynaptic membranes on apical dendritic shafts of CA1 pyramidal neurons in aged rats, it had

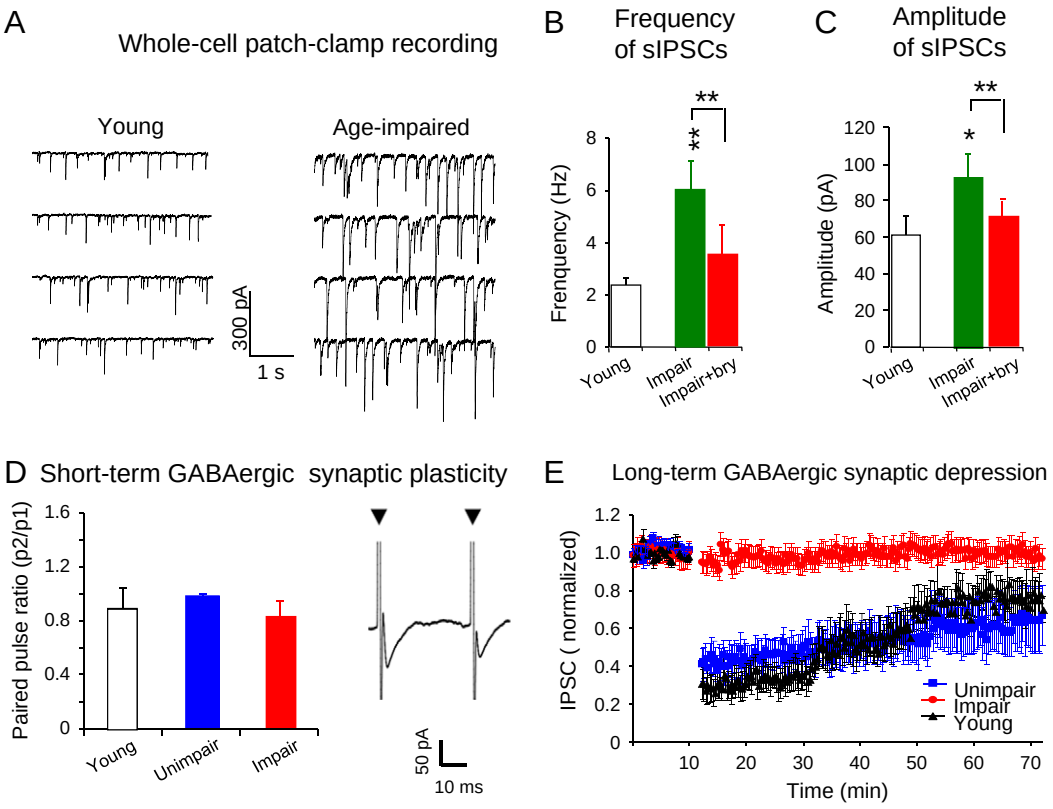

Fig. 7. Bryostatin treatment during spatial memory training restores frequency and amplitude of spontaneous inhibitory postsynaptic currents in aged-impaired rats. Electrophysiology was conducted at 24 h after memory retention was evaluated (Fig. 2A). (A) Traces of sIPSCs were obtained by whole-cell patch-clamp recording. Aged-impaired rats showed increases in (B) frequency and (C) amplitude of sIPSCs, which were reduced by bryostatin treatment. (D) The alteration of short-term GABAergic synaptic plasticity with aging. Paired-pulse recording interval is 50 ms. (E) The alteration of long-term GABAergic synaptic depression with aging. Long-term depression (I-LTD) was impaired in aged-impaired animals. Data are presented as mean ± SEM; $^{*}P < 0.05$. $^{**}P < 0.01$; paired t-test. Asterisks over bars, compared with young; asterisks over brackets, comparison of untreated and treated animals in each group. Unimpair = aged, learning-unimpaired; impair = aged, learning-impaired; bry = bryostatin.

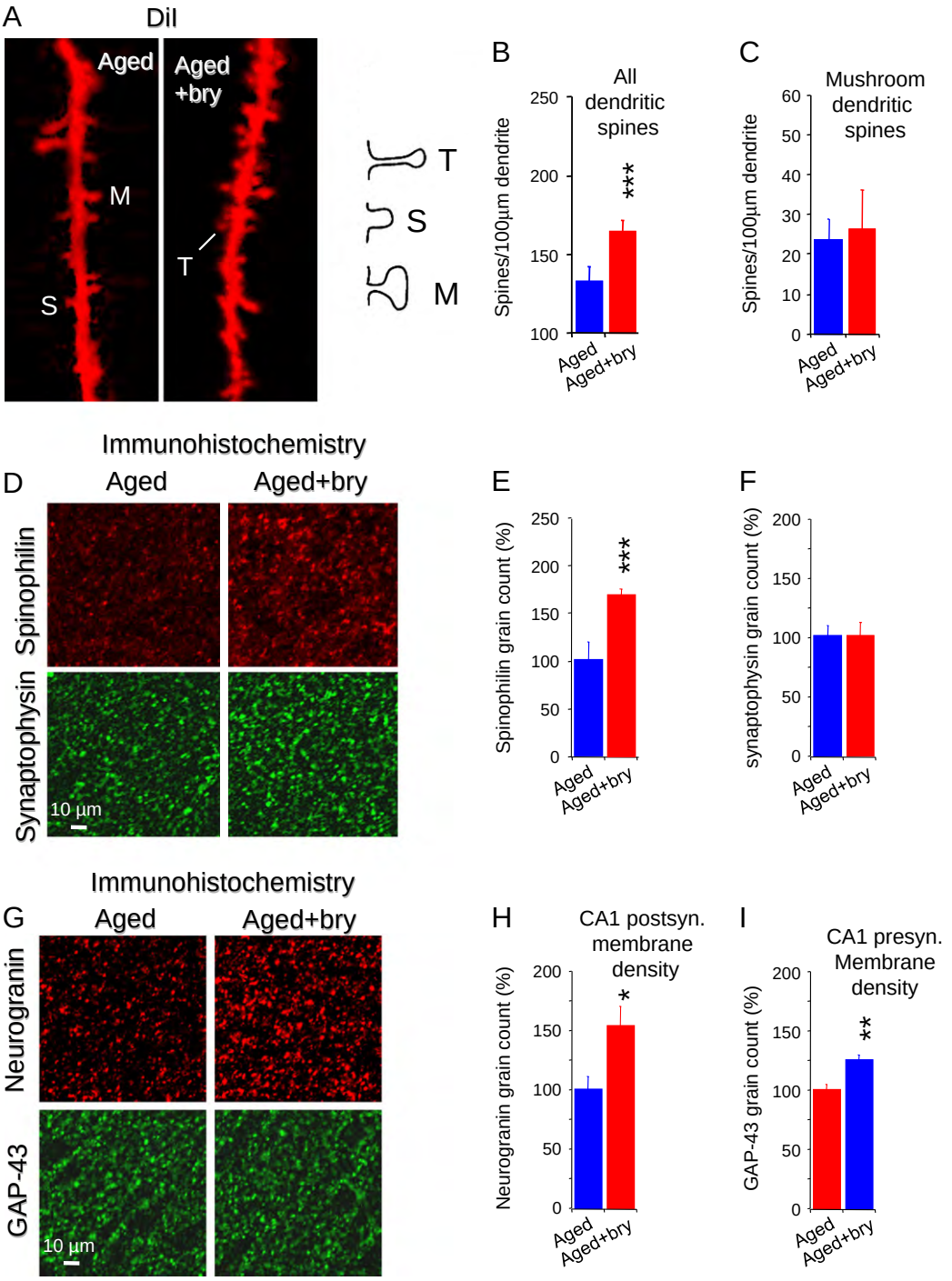

Fig. 8. Bryostatin increases non-mushroom dendritic spines and pre- and postsynaptic membrane density in aged rats without spatial memory training. (A) DiI staining and confocal microscopy show distinct shapes of dendritic spines: mushroom (M), thin (T), and stubby (S). The number of spines per 100 µm apical dendritic shaft of CA1 pyramidal neurons was determined by serial scanning and 3D reconstruction. (B) All-shape, but not (C) mushroom, dendritic spines in aged rats increased with bryostatin treatment (5 µg/kg body wt., i.p., 3 doses every other day for 6 days). (D) By immunostaining and confocal microscopy, bryostatin increased (E) postsynaptic dendritic spines (spinophilin) and (F) presynaptic axonal boutons (synaptophysin). (G) By immunocytochemistry and confocal microscopy, bryostatin increased (H) postsynaptic membranes (neurogranin) on and (I) presynaptic membranes (GAP-43). Data in E, F, H and I are reported per $63 \times 63 \times 0.6\ \mu m^3$ of stratum radiatum. Confocal images at 0.6-µm thickness were used to ensure that each counted grain represented only 1 presynaptic or postsynaptic structure, and not an overlay of more than 2 structures. Data are presented as mean ± SEM; $^{*}P < 0.05$, $^{**}P < 0.01$, $^{***}P < 0.001$; two-tailed t-test. bry = bryostatin.

no effect on mushroom dendritic spine formation, which is specifically induced during memory retention. The results also suggest that bryostatin without water maze training increased non-mushroom dendritic spines that formed multiple synapses with the existing axonal boutons.

Discussion

The objective of the present study was to examine age-related decline in cognitive function (spatial memory) and associated changes at behavioral, structural, molecular, and electrophysiological levels in

the hippocampal circuit, and whether PKC activation could reverse these changes. During learning, highly processed multi-modal information converges from cortical association areas to the entorhinal cortex, which communicates with the hippocampal dentate gyrus and CA3, CA2, and CA1 areas for memory processing. Consistent with our previous findings (Hongpaisan and Alkon, 2007), we found that although the PKC activator bryostatin itself was able to increase the density of the total number of all dendritic spines in CA1 pyramidal neurons of aged, learning-impaired rats, the number of mushroom spines was unchanged. This led us to hypothesize that the combination of PKC activation and spatial memory training might enhance mushroom spine synapse formation and improve cognitive function in aged animals.

In mature brains, thin spines transiently emerge and disappear over time (Bourne and Harris, 2007; Kasai et al., 2010), and are considered to be "learning spines" because they can enlarge in response to synaptic activity. In contrast, mushroom spines are more stable and are considered to be "memory spines." Mushroom spines make up less than 20% of the total number of dendritic spines (Beltran-Campos et al., 2011; Harris et al., 1992).

Behavioral learning and memory training (by trace eyeblink conditioning) increase the number of perforated PSDs, which are found primarily on mushroom dendritic spines (Geinisman et al., 2000). At 24 h after fear-conditioning learning, new AMPA receptors are selectively synthesized and recruited to mushroom spines in adult hippocampal neurons (Matsuo et al., 2008). Our study (Figs. 2D, 3C) confirmed previous work demonstrating that a ≥2-fold increase in the number of mushroom spines in the apical dendrites of hippocampal CA1 pyramidal neurons correlates with spatial memory induced by water maze training (Beltran-Campos et al., 2011; Hongpaisan and Alkon, 2007). Conversely, the loss of mushroom dendritic spines and synapses – in aged learning-impaired rats (Figs. 2D, 3C) and in ovariectomized animals (Beltran-Campos et al., 2011) – correlates with spatial memory impairment after water maze training.

We do not yet know the threshold number of mushroom spines below which memory deficits become evident, or the level of mushroom spinogenesis that must be reached to restore memory function. Nevertheless, we have found that PKC activators can completely (100%) restore or prevent the loss of mushroom spine synaptogenesis induced by water maze training in age-dependent memory-impaired rats (present study), in a cerebral ischemia/hypoxia rat model (Sun et al., 2009), and in a transgenic mouse model of Alzheimer's disease (Hongpaisan et al., 2011). Others have shown that in ovariectomized mice, 1 μg of estradiol benzoate for 5 days enhanced objective placement spatial memory and increased mushroom spine density 38% (Li et al., 2004).

Previous studies have assessed long-term age-associated morphological changes in the hippocampal circuit at 1 month after water maze training (e.g., Geinisman et al., 2004); however, the impact of aging on recent memory is also a meaningful endpoint for day-to-day living in senior citizens. Here, we performed morphological and biochemical studies 24 h after memory had been established, as determined with a probe test 24 h after the second water maze training period (Vorhees and Williams, 2006). The present study demonstrates age-related effects on recent memory plasticity induced by spatial learning, and restoration of memory with the addition of bryostatin treatment.

In aged rats with recent memory decline, we showed lower presynaptic PKCε expression in the axon bundle of granule cells in the dentate gyrus (the mossy fibers) to the CA3 pyramidal neurons, impaired presynaptic PKCε signaling in the axonal boutons of the CA3 pyramidal neuron axons (the Schaffer collateral fibers) to the CA1 pyramidal neurons, and lower postsynaptic PKCα signaling in the CA1 pyramidal neuron cell bodies. Importantly, these biochemical changes correlated with a lower mushroom spine density and lower synaptic density on the apical dendrites of CA1 pyramidal neurons as well as memory impairment in aged, learning-impaired animals.

Our findings of reduced PKCε expression and signaling are consistent with previous studies that describe reduced expression of BDNF mRNA, protein, and its receptor during aging (Chapman et al., 2012; von Bohlen und Halbach, 2010; Walker et al., in press). BDNF can increase the postsynaptic density-95 (PSD-95) protein, a marker for synaptic strength, in dendritic spines (Hu et al., 2011) and induce mushroom spine formation (Chapleau et al., 2008). We recently found that bryostatin treatment promotes the association of HuD with target mRNAs, including BDNF (C.S. Lim and D.L. Alkon, unpublished observations). PKCε expression is selectively higher in axons and presynaptic sites (Shirai et al., 2008) and may influence presynaptic HuD activity (Akten et al., 2011). Taken together, our results suggest that the hippocampal CA3–CA1 connection is altered during aging such that the combined loss of PKCε-containing presynaptic boutons, HuD activity, and PKCε-dependent local BDNF protein synthesis negatively impacts the formation of mushroom spine synapses and memory retention.

In aged animals, several groups have reported a reduction in plasma membrane translocation and activation of PKC due to decreased expression of the PKC anchoring protein RACK1 (Battaini and Pascale, 2005; Govoni et al., 2010). In the present study, we correlated reduced PKCα levels in the hippocampi of rats with age-related memory impairment, and confirmed a significant reduction in PKCα in the cell bodies of CA1 dorsal pyramidal neurons by immunohistochemistry. By contrast, Colombo et al (1997) reported no reduction in PKCα by immunoblot analysis in aged, learning-impaired Long–Evans rats with cognitive evaluation. The basis for this discrepancy is unknown, but may be due to the use of different rat strains. In our experience, brown Norway rats learn slowly and require prolonged training to achieve memory retention. When comparing the learning curves of aged, learning impaired brown Norway rats and Long–Evans rats used by Colombo et al (1997), the brown Norway rats showed a prolonged latency time, suggesting a greater degree of age-related memory impairment. Other groups have also reported no changes in PKCα expression by immunoblot analysis of the hippocampi of aged animals without behavioral training to differentiate their cognitive performance (Govoni et al., 2010; Pascale et al., 2005; Van der Zee et al., 2004). This may be due to the fact that data were pooled from aged-unimpaired (without PKCα reduction, data not shown in this study) and aged-impaired (with PKCα reduction) rats, resulting in no apparent PKCα reduction. Furthermore, using immunohistochemistry and optical analysis, Van der Zee et al (1997, 2004) demonstrated in aged rats without cognitive evaluation that there was no change in PKCα levels in the CA1 stratum pyramidale at the level of multiple pyramidal neuron cell bodies (including supporting cells), but the number of PKCα-containing interneurons was significantly lower upon single cell level analysis in the CA1 stratum oriens area. These data suggest that single cell measurement by immunohistochemistry is more sensitive than multiple cell measurement for detecting differences in PKC expression.

Loss of PKCγ or PKCβ in knockout mice leads to moderate memory deficits (Abeliovich et al., 1993; Weeber et al., 2000); however, we demonstrated that a specific PKCε activator, DCP-LA, when added to spatial memory training, is sufficient to restore synaptic spine density in aged, learning-impaired rats, suggesting that deficiencies in the PKCε isozyme may be more highly correlated to the loss of synaptic formation at CA3-to-CA1 neuron connection in aging.

Our study demonstrated that PKC activators increase the expression of PKCε and PKCα and restored PKCε and PKCα signaling, which was associated with an increase in mushroom dendritic spinogenesis and synaptogenesis in CA1 pyramidal neurons, as well as improved spatial memory retention in aged rats. We also observed that activation of PKCε and PKCα by bryostatin could induce PKC expression, consistent with our previous study (Hongpaisan et al., 2011); however, it is unknown whether the effect of bryostatin on PKCε and PKCα

protein levels involves de novo gene transcription or translation of pre-existing mRNAs.

Our findings are also consistent with the view that age-related decline in cognitive function is not related to hippocampal neuronal loss, but to discrete physiologic and morphologic changes of dendritic spines and synapses in the hippocampal circuitry (Burke and Barnes, 2006; Wilson et al., 2006). Previous studies have described a loss of axospinous synapses between axonal boutons of axons from the entorhinal cortex and dendritic spines of granule cells in the hippocampal dentate gyrus (Geinisman et al., 1992), as well as in humans with mild cognitive impairment (Scheff et al., 2006). Magnetic resonance imaging has revealed marked atrophy in the perforant path of aged, memory-impaired humans (Kalus et al., 2006). These changes were thought to lead to a significant reduction in the perforant path excitatory synaptic potential (Barnes and McNaughton, 1980); however, aged granule cells exhibit strong depolarization in response to perforant path stimulation, likely due to an increase in quantal size or synaptic efficacy that compensates for the reduced number of synapses (Foster et al., 1991).

During aging, neuronal dysfunction in the prefrontal cortex has been implicated in working memory decline (Wang et al., 2011). In contrast to the hippocampus, working memory decline during aging is the result of the overactivation of PKC and synaptic loss in the prefrontal cortex (Brennan et al., 2009). In addition, electrophysiological and anatomical studies have shown that the primary cortical extrinsic input through the entorhinal cortex to the dentate gyrus and the CA3 area of the hippocampus is substantially reduced, due to a decrease in either presynaptic bouton number and/or vesicle concentration (Gallagher et al., 2003; Smith et al., 2000). The present study clarifies the age-related presynaptic biochemical changes (e.g., reduced PKCε) that occur in axons of dentate gyrus granule cells to CA3 pyramidal neurons. However, the intrinsic auto-associative connections between the dentate gyrus-to-CA3 and within CA3 axons are spared during aging (Lister and Barnes, 2009; Wilson et al., 2006). This may be due to the compensation caused by reduced (inhibitory) modulation from the medium septum, which provides the major cholinergic innervation to the dentate gyrus, CA3, and CA1 areas (Wilson et al., 2006).

Despite the lack of evidence of synaptic loss (Calhoun et al., 1998; Geinisman et al., 2004; Phinney et al., 1999) or age-related changes in presynaptic fiber electrophysiologic potentials (Barnes et al., 1997, 2000; Rosenzweig et al., 1997) from the CA3 to CA1 neurons, a decrease in the field excitatory postsynaptic potential (EPSP) and an increase in sIPSC have been observed in CA1 pyramidal neurons of aged, learning-impaired animals (Barnes et al., 1992; Peters et al., 2008). These findings have led some to suggest that, during aging, a subset of hippocampal synapses becomes non-functional or silent (Sametsky et al., 2010) and/or there is a reduction in axospinous perforated PSD that leads to decreased postsynaptic activity of CA1 pyramidal neurons (Hussain and Carpenter, 2003; Nicholson et al., 2004). Given that PKC is important for CA3-to-CA1 synaptic transmission (Grabauskas et al., 2006; Hussain and Carpenter, 2003), our work suggests that age-related reductions in presynaptic PKCε levels and activity, and an increase in sIPSC, may contribute to the decrease in the function of CA1 pyramidal neurons and decreased formation of mushroom dendritic spines and synapses after spatial memory training.

Physical training can activate synaptogenesis and is a critical component of treatment for age-related memory impairment (Ahlskog et al., 2011; Kraft, 2012). Likewise, late phase motor skill learning can induce cortical synaptogenesis (Kleim et al., 2004). Previous studies have also implicated that estrogen may increase synapse formation; estrogen induced synaptic proteins in cultured neurons and in the brains of ovariectomized adult and aged female animals (Chisholm and Juraska, 2012; Jelks et al., 2007; Yankova et al., 2001). In the present study, we showed that PKC activation during spatial memory training could stimulate mushroom spinogenesis and synaptogenesis in aged male rats. Pharmacologic approaches using PKC activators have successfully prevented the loss of synapses under various neurodegenerative conditions (Hongpaisan et al., 2011; Sun et al., 2008). A better understanding of the mechanisms and pathways that reverse the morphologic and functional changes that occur in synapses in various neurodegenerative diseases and conditions, including normal aging, may reveal new targets for treatments that can restore lost synaptogenesis and cognitive function.

Conclusions

In summary, we found that aged, learning-impaired rats have lower memory retention; fewer mushroom spines and mushroom spine synapse densities in the apical dendrites of CA1 pyramidal neurons; fewer PKCε-containing CA3 axonal boutons; and lower levels of activated BDNF and HuD expression. Bryostatin treatment without spatial memory training increased the number of non-mushroom spine synapses. Treatment with bryostatin combined with spatial memory training of aged, learning-impaired rats restored PKCε and α expression, HuD activity, and BDNF expression; restored mushroom spinogenesis and synaptogenesis; and normalized memory retention to the levels seen in young rats. These results demonstrate that PKC activation enhances the effects of spatial memory training on mushroom spine synaptogenesis in the aging brain, and supports the therapeutic potential of PKC activators together with cognitive training for reversing synaptic loss and memory decline in various neurodegenerative diseases and conditions.

Abbreviations

DiI	1,1′-Dioctadecyl-3,3,3′,3′-tetramethylindocarbocyanine perchlorate
GAP-43	growth-associated protein-43/B-50
PBS	phosphate buffered saline
PSD	postsynaptic density
sEPSCs	spontaneous excitatory amino acid currents

Supplementary data to this article can be found online at http://dx.doi.org/10.1016/j.nbd.2013.03.012.

Acknowledgments

We are indebted to Dr. Stacey Tobin and Darryl DeNuto for assisting in the preparation of this manuscript and Wen Zheng for technical assistance.

References

Abeliovich, A., Paylor, R., Chen, C., Kim, J.J., Wehner, J.M., Tonegawa, S., 1993. PKCγ mutant mice exhibit mild deficits in spatial and contextual learning. Cell 75, 1263–1271.
Ahlskog, J.E., Geda, Y.E., Graff-Radford, N.R., Petersen, R.C., 2011. Physical exercise as a preventive or disease-modifying treatment of dementia and brain aging. Mayo Clin. Proc. 86, 876–884.
Akten, B., Kye, M.J., Hao, L.T., Wertz, M.H., Singh, S., Nie, D., Huang, J., Merianda, T.T., Twiss, J.L., Beattie, C.E., Steen, J.A., Sahin, M., 2011. Interaction of survival of motor neuron (SMN) and HuD proteins with mRNA cpg15 rescues motor neuron axonal deficits. Proc. Natl. Acad. Sci. U. S. A. 108, 10337–10342.
Antic, D., Keene, J.D., 1998. Messenger ribonucleoprotein complexes containing human ELAV proteins: interactions with cytoskeleton and translational apparatus. J. Cell Sci. 111, 183–197.
Aranda-Abreu, G.E., Behar, L., Chung, S., Furneaux, H., Ginzburg, I., 1999. Embryonic lethal abnormal vision-like RNA-binding proteins regulate neurite outgrowth and tau expression in PC12 cells. J. Neurosci. 19, 6907–6917.
Bank, B., Deweer, A., Kuzirian, A.M., Ramussen, H., Alkon, D.L., 1988. Classical conditioning induces long-term translocation of protein kinase C in rabbit hippocampal CA1 Cells. Proc. Natl. Acad. Sci. U. S. A. 85, 1988–1992.
Barnes, C.A., McNaughton, B.L., 1980. Physiological compensation for loss of afferent synapses in rat hippocampal granule cells during senescence. J. Physiol. 309, 473–485.
Barnes, C.A., Rao, G., Foster, T.C., McNaughton, B.L., 1992. Region-specific age effects on AMPA sensitivity: electrophysiological evidence for loss of synaptic contacts in hippocampal field CA1. Hippocampus 2, 457–468.

Barnes, C.A., Rao, G., Shen, J., 1997. Age-related decrease in the N-methyl-D-aspartateR-mediated excitatory postsynaptic potential in hippocampal region CA1. Neurobiol. Aging 18, 445–452.
Barnes, C.A., Rao, G., Orr, G., 2000. Age-related decrease in the Schaffer collateral-evoked EPSP in awake, freely behaving rats. Neural Plast. 7, 167–178.
Battaini, F., Pascale, A., 2005. Protein kinase C signal transduction regulation in physiological and pathological aging. Ann. N. Y. Acad. Sci. 1057, 177–192.
Beltran-Campos, V., Prado-Alcala, R.A., Leon-Jacinto, U., Aguilar-Vazques, A., Quirarte, G.L., Ramirez-Amaya, V., Diaz-Cintra, S., 2011. Increase of mushroom spine density in CA1 apical dendrites produced by water maze training is prevented by ovariectomy. Brain Res. 1369, 119–130.
Bourne, J., Harris, K.M., 2007. Do thin spines learn to be mushroomspines that remember? Curr. Opin. Neurobiol. 17, 381–386.
Brennan, A.B., Yuan, P., Dickstein, D.L., Rocher, A.B., Hof, P.R., Maniji, H., Arnsten, F.T., 2009. Protein kinase C activity is associated with prefrontal cortical decline in aging. Neurobiol. Aging 30, 782–792.
Burke, S.N., Barnes, C.A., 2006. Neural plasticity in the ageing brain. Nat. Rev. Neurosci. 7, 30–40.
Calhoun, M.E., Kurth, D., Phinney, A.L., Long, J.M., Hengemihle, J., Mouton, P.R., Ingram, D.K., Jucker, M., 1998. Hippocampal neuron and synaptophysin-positive bouton number in aging C57BL/6 mice. Neurobiol. Aging 19, 599–606.
Chapleau, C.A., Carlo, M.E., Larimore, J.L., Pozzo-Miller, L., 2008. The actions of BDNF on denritic spine density and morphology in organotypic slice cultures depend on the presence of serum in culture media. J. Neurosci. Methods 169, 182–190.
Chapman, T.R., Barrientos, R.M., Ahrendsen, J.T., Hoover, J.M., Maier, S.F., Patterson, S.L., 2012. Aging and infection reduce expression of specific brain-derived neurotrophic factor mRNAs in hippocampus. Neurobiol. Aging 33 (832), e1–e14.
Chisholm, N.C., Juraska, J., 2012. Effects of long-term treatment with estrogen and medroxyprogesterone acetate on synapse number in the medial prefrontal cortex of aged female rats. Menopause 19 (7), 804–811.
Chung, S., Eckrich, M., Perrone-Bizzozero, N., Kohn, D.T., Furneaux, H., 1997. The ELAV-like proteins bind to a conserved regulatory element in the 3′-untranslated region of GAP-43 mRNA. J. Biol. Chem. 272, 6593–6598.
Colombo, P.J., Wetsel, W.C., Gallagher, M., 1997. Spatial memory is related to hippocampal subcellular concentrations of calcium-dependent protein kinase C isoforms in young and aged rats. Proc. Natl. Acad. Sci. U. S. A. 94, 14195–14199.
Foster, T.C., Barnes, C.A., Rao, G., McNaughton, B.L., 1991. Increase in perforant path quantal size in aged F-344 rats. Neurobiol. Aging 12, 441–448.
Gallagher, M., Bizon, J.L., Hoyt, E.C., Helm, K.A., Lund, P.K., 2003. Effects of aging on the hippocampal formation in a naturally occurring animal model of mild cognitive impairment. Exp. Gerontol. 38, 71–77.
Geinisman, Y., deToledo-Morrell, L., Morrell, F., Persina, I.S., Rossi, M., 1992. Age-related loss of axospinous synapses formed by two afferent systems in the rat dentate gyrus as revealed by the unbiased stereological dissector technique. Hippocampus 2, 437–444.
Geinisman, Y., Disterhoft, J.F., Gundersen, H.J., McEchron, M.D., Persina, I.S., Power, J.M., van der Zee, E.A., West, M.J., 2000. Remodeling of hippocampal synapses after hippocampus-dependent associative learning. J. Comp. Neurol. 417, 49–59.
Geinisman, Y., Ganeshina, O., Yoshida, R., Berry, R.W., Disterhoft, J.F., Gallagher, M., 2004. Aging, spatial learning, and total synapse number in the rat CA1 stratum radiatum. Neurobiol. Aging 25, 407–416.
Govoni, S., Amadio, M., Battaini, F., Pascale, A., 2010. Senescence of the brain: focus on cognitive kinases. Curr. Pharm. Des. 16, 660–671.
Grabauskas, G., Chapman, H., Wheal, H.V., 2006. Role of protein kinase C in modulation of excitability of CA1 pyramidal neurons in the rat. Neuroscience 139, 1301–1313.
Hama, H., Hara, C., Yamaguchi, K., Miyawaki, A., 2004. PKC signaling mediates global enhancement of excitatory synaptogenesis in neurons triggered by local contact with astrocytes. Neuron 41, 405–415.
Hara, Y., Park, C.S., Janssen, W.G.M., Roberts, M.T., Morrison, J.H., Rapp, P.R., 2012. Synaptic correlates of momory and menopause in the hippocampal dentate gyrus in rhesus monkeys. Neurobiol. Aging 33 (421), e17–e28.
Harris, K.M., Jensen, F.E., Tsao, B., 1992. Three-dimensional structure of dendritic spines and synapses in rat hippocampus (CA1) at postnatal day 15 and adult ages: implications for the maturation of synaptic physiology and long-term potentiation. J. Neurosci. 12, 2685–2705.
Hof, P.R., Morrison, J.H., 2004. The aging brain: morphomolecular senescence of cortical circuits. Trends Neurosci. 27, 607–613.
Hongpaisan, J., Alkon, D.L., 2007. A structural basis for enhancement of long-term associative memory in single dendritic spines regulated by PKC. Proc. Natl. Acad. Sci. U. S. A. 104, 19571–19576.
Hongpaisan, J., Sun, M.K., Alkon, D.L., 2011. PKC epsilon activation prevents synaptic loss, Abeta elevation, and cognitive deficits in Alzheimer's disease transgenic mice. J. Neurosci. 31, 630–643.
Hu, X., Ballo, L., Pietila, L., Viesselmann, C., Ballweg, J., Lumbard, D., Stevenson, M., Merriam, E., Dent, E.W., 2011. BDNF-induced increase of PSD-95 in dendritic spines requires dynamic microtubule invasions. J. Neurosci. 31, 15597–15603.
Hussain, R.J., Carpenter, D.O., 2003. The effects of protein kinase C activity on synaptic transmission in two areas of rat hippocampus. Brain Res. 990, 28–37.
Jelks, K.B., Wylie, R., Floyd, C.L., AcAlilister, K., Wise, P., 2007. Estradiol targets synaptic proteins to induce glutamatergic synapse formation in cultured hippocampal neurons: critical role of estrogen receptor-α. J. Neurosci. 27, 6903–6913.
Kalus, P., Slotboom, J., Gallinat, J., Mahlberg, R., Cattapan-Ludewig, K., Wiest, R., Nyffeler, T., Buri, C., Federspiel, A., Kunz, D., Schroth, G., Kiefer, C., 2006. Examining the gateway to the limbic system with diffusion tensor imaging: the perforant pathway in dementia. NeuroImage 30, 713–720.
Kasai, H., Fukuda, M., Watanabe, S., Hayashi-Takagi, A., Noguchi, J., 2010. Structural dynamics of dendritic spines in memory and cognition. Cell 33, 121–129.
Kirov, S.A., Petrak, L.J., Fiala, J.C., Harris, K.M., 2004. Dendritic spines disappear with chilling but proliferate excessively upon rewarming of mature hippocampus. Neuroscience 127, 69–80.
Kleim, J.A., Hogg, T.M., VanderBerg, P.M., Cooper, N.R., Bruneau, R., Remple, M., 2004. Cortical synaptogenesis and motor map reorganization occur during late, but not early, phase of motor skill learning. J. Neurosci. 24, 628–633.
Kraft, E., 2012. Cognitive function, physical activity, and aging: possible biological links and implication for multimodal interventions. Neuropsychol. Dev. Cogn. Aging Neuropsychol. Cogn. 19, 248–263.
Li, C., Brake, W.G., Romeo, R.D., Dunlop, J.C., Gordon, M., Buzescu, R., Magarinos, A., Allen, P., Greengard, P., Luine, V., McEwen, B.S., 2004. Estrogen alters hippocampal dendritic spine shape and enhances synaptic protein immunoreactivity and spatial memory tasks in female mice. Proc. Natl. Acad. Sci. U. S. A. 101, 2185–2190.
Lister, J.P., Barnes, C.A., 2009. Neurobiological changes in the hippocampus during normative aging. Arch. Neurol. 66, 829–833.
Luebke, J.I., Chang, Y.M., Moore, T.L., Rosene, D.L., 2004. Normal aging results in decreased synaptic excitation and increased synaptic inhibition of layer 2/3 pyramidal cells in the monkey prefrontal cortex. Neuroscience 125, 277–288.
Matsuo, N., Reijmers, L., Mayford, M., 2008. Spine-type-specific recruitment of newly synthesized AMPA receptors with learning. Science 319, 1104–1107.
Mattews, S.A., Pettit, G.R., Rozengurt, E., 1997. Bryostatin-1 induces biphasic activation of protein kinase D in intact cells. J. Biol. Chem. 272, 20245–20250.
Miranda, R., Blanco, E., Begega, A., Santin, L.J., Arias, J.L., 2006. Reversible changes in hippocampal CA1 synapses associated with water maze training in rats. Synapse 59, 177–181.
Moser, M.B., Trommald, M., Andersen, P., 1994. An increase in dendritic spine density on hippocampal CA1 pyramidal cells following spatial learning in adult rats suggests the formation of new synapses. Proc. Natl. Acad. Sci. U. S. A. 91, 12673–12675.
Mutter, R., Wills, M., 2000. Chemistry and clinical biology of the bryostatins. Bioorg. Med. Chem. 8, 1841–1860.
Nelson, T.J., Cui, C., Luo, Y., Alkon, D.L., 2009. Reduction of beta-amyloid levels by novel protein kinase Cε activators. J. Biol. Chem. 284, 34514–34521.
Nicholson, D.A., Yoshida, R., Berry, R.W., Gallagher, M., Geinisman, Y., 2004. Reduction in size of perforated postsynaptic densities in hippocampal axospinous synapses and age-related spatial learning impairments. J. Neurosci. 24, 7648–7653.
Nicholson, D.A., Trana, R., Katz, Y., Kath, W.L., Spruston, N., Geinisman, Y., 2006. Distance-dependent differences in synapse number and AMPA receptor expression in hippocampal CA1 pyramidal neurons. Neuron 50, 431–442.
Nilsson, L.G., 2003. Memory function in normal aging. Acta Neurol. Scand. Suppl. 179, 7–13.
Olds, J.L., Anderson, M.L., McPhie, D.L., Staten, L.D., Alkon, D.L., 1989. Imaging of memory-specific changes in the distribution of protein kinase c in the hippocampus. Science 245, 866–869.
Pascale, A., Gusev, P.A., Amadio, M., Dottorini, T., Govoni, S., Alkon, D.L., Quattrone, A., 2004. Increase of the RNA-binding protein HuD and posttranscriptional up-regulation of the GAP-43 gene during spatial memory. Proc. Natl. Acad. Sci. U. S. A. 101, 1217–1222.
Pascale, A., Amadio, M., Scapagnini, G., Lanni, C., Racchi, M., Provenzani, A., Govoni, S., Alkon, D.L., Quattrone, A., 2005. Neuronal ELAV proteins enhance mRNA stability by a PKCalpha-dependent pathway. Proc. Natl. Acad. Sci. U. S. A. 102, 12065–12070.
Perrone-Bizzozero, N., Bolognani, F., 2002. Role of HuD and other RNA-binding proteins in neural development and plasticity. J. Neurosci. Res. 68, 121–126.
Peters, A., Sethares, C., Luebke, J.I., 2008. Synapses are lost during aging in the primate prefrontal cortex. Neuroscience 152, 970–981.
Phinney, A.L., Calhoun, M.E., Wolfer, D.P., Lipp, H.P., Zheng, H., Jucker, M., 1999. No hippocampal neuron or synaptic bouton loss in learning-impaired aged beta-amyloid precursor protein-null mice. Neuroscience 90, 1207–1216.
Prekeris, R., Mayhew, M.W., Cooper, J.B., Terrian, D.M., 1996. Identification and localization of an actin-binding motif that is unique to the epsilon isoform of protein kinase C and participates in the regulation of synaptic function. J. Cell Biol. 132, 77–90.
Quattrone, A., Pascale, A., Nogues, X., Zhao, W., Gusev, P., Pacini, A., Alkon, D.L., 2001. Post-transcriptional regulation of gene expression in learning by the neuronal ELAV-like mRNA-stabilizing proteins. Proc. Natl. Acad. Sci. U. S. A. 98, 11668–11673.
Rapp, P.R., Gallagher, M., 1996. Preserved neuron number in the hippocampus of aged rats with spatial learning deficits. Proc. Natl. Acad. Sci. U. S. A. 93, 9926–9930.
Rodriguez, A., Ehlenberger, D.B., Dickstein, D.L., Hof, P.R., Wearne, S.L., 2008. Automated three-dimensional detection and shape classification of dendritic spines from fluorescence microscopy images. PLoS One 3, e1997.
Rodriguez-Moreno, A., Lopez-Garcia, J.C., Lerma, J., 2000. Two populations of kainate receptors with separate signaling mechanisms in hippocampal interneurons. Proc. Natl. Acad. Sci. U. S. A. 97, 1293–1298.
Rosenzweig, E.S., Rao, G., McNaughton, B.L., Barnes, C.A., 1997. Role of temporal summation in age-related long-term potentiation–induction deficits. Hippocampus 7, 549–558.
Rusakov, D.A., Davies, H.A., Harrison, E., Diana, G., Richter-Levin, G., Bliss, T.V., Stewart, M.G., 1997. Ultrastructural synaptic correlates of spatial learning in rat hippocampus. Neuroscience 80, 69–77.
Sametsky, E.A., Disterhoft, J.F., Geinisman, Y., Nicholson, D.A., 2010. Synaptic strength and postsynaptically silent synapses through advanced aging in rat hippocampal CA1 pyramidal neurons. Neurobiol. Aging 31, 813–825.
Scheff, S.W., Price, D.A., Schmitt, F.A., Mufson, E.J., 2006. Hippocampal synaptic loss in early Alzheimer's disease and mild cognitive impairment. Neurobiol. Aging 27, 1372–1384.
Shirai, Y., Adachi, N., Saito, N., 2008. Protein kinase C epsilon: function in neurons. FEBS J. 275, 3988–3994.

Shrager, Y., Bayley, P.J., Bontempi, B., Hopkins, R.O., Squire, L.R., 2007. Spatial memory and the human hippocampus. Proc. Natl. Acad. Sci. U. S. A. 104, 2961–2966.
Smith, M.L., Milner, B., 1981. The role of the right hippocampus in the recall of spatial location. Neuropsychologia 19, 781–793.
Smith, T.D., Adams, M.M., Gallagher, M., Morrison, J.H., Rapp, P.R., 2000. Circuit-specific alterations in hippocampal synaptophysin immunoreactivity predict spatial learning impairment in aged rats. J. Neurosci. 20, 6587–6593.
Sorra, K.E., Harris, K.M., 2000. Overview on the structure, composition, function, development, and plasticity of hippocampal dendritic spines. Hippocampus 10, 501–511.
Sun, M.K., Hongpaisan, J., Nelson, T.J., Alkon, D.L., 2008. Poststroke neuronal rescue and synaptogenesis mediated in vivo by protein kinase C in adult brains. Proc. Natl. Acad. Sci. U. S. A. 105, 13620–13625.
Sun, M.K., Hongpaisan, J., Alkon, D.L., 2009. Postischemic PKC activation rescues retrograde and anterograde long-term memory. Proc. Natl. Acad. Sci. U. S. A. 106, 14676–14680.
Tao-Cheng, J.H., Gallant, P.E., Brightman, M.W., Dosemeci, A., Reese, T.S., 2007. Structural changes at synapses after delayed perfusion fixation in different regions of the mouse brain. J. Comp. Neurol. 501, 731–740.
Uttl, B., Graf, P., 1993. Episodic spatial memory in adulthood. Psychol. Aging 8, 257–273.
Van der Zee, E.A., Kronforst-Collins, M.A., Maizels, E.T., Hunzicker-Dunn, M., Disterhoft, J.F., 1997. Gamma isoform-selective changes in PKC immunoreactivity after trace eyeblink conditioning in the rabbit hippocampus. Hippocampus 7, 271–285.
Van der Zee, E.A., Palm, I.F., O'Connor, M., Maizels, E.T., Hunzicker-Dunn, M., Disterhoft, J.F., 2004. Aging-related alterations in the distribution of Ca^{2+}-dependent PKC isoforms in rabbit hippocampus. Hippocampus 14, 849–860.
von Bohlen und Halbach, O., 2010. Involvement of BDNF in age-dependent alterations in the hippocampus. Front. Aging Neurosci. 36, 1–11.
Vorhees, C.V., Williams, M.T., 2006. Morris water maze: procedures for assessing spatial and related forms of learning and memory. Nat. Protoc. 1, 848–858.
Walker M.P., LaFerla F.M., Oddo S.S., Brewer G.J., in press. Reversible epigenetic histone modifications and BDNF expression in neurons with aging and from a mouse model of Alzheimer's disease. Age (Dordr).
Wang, M., Gamo, N.J., Yang, Y., Jin, L.E., Wang, X.J., Laubach, M., Mazer, J.A., Lee, D., Arnsten, A.F., 2011. Neuronal basis of age-related working memory decline. Nature 476, 210–213.
Weeber, E.J., Atkins, C.M., Selcher, J.C., Varga, A.W., Mirnikjoo, B., Paylor, R., Leitges, M., Sweatt, J.D., 2000. J. Neurosci. 20, 5906–5914.
Wilkniss, S.M., Jones, M.G., Korol, D.L., Gold, P.E., Manning, C.A., 1997. Age-related differences in an ecologically based study of route learning. Psychol. Aging 12, 372–375.
Wilson, I.A., Gallagher, M., Eichenbaum, H., Tanila, H., 2006. Neurocognitive aging: prior memories hinder new hippocampal encoding. Trends Neurosci. 29, 662–670.
Wu, M., Zhang, Z., Leranth, C., Xu, C., van den Pol, A.N., Alreja, M., 2002. Hypocretin increases impulse flow in the septohippocampal GABAergic pathway: implications for arousal via a mechanism of hippocampal disinhibition. J. Neurosci. 22, 7754–7765.
Xu, C., Cui, C., Alkon, D.L., 2009. Age-dependent enhancement of inhibitory synaptic transmission in CA1 pyramidal neurons via GluR5 kainate receptors. Hippocampus 19, 706–717.
Yankova, M., Hart, S.A., Wooley, C.S., 2001. Estrogen increases synaptic connectivity between single presynaptic inputs and multiple postsynaptic CA1 pyramidal cells: a serial electron-microscopy study. Proc. Natl. Acad. Sci. U. S. A. 98, 3525–3530.
Zhang, X., Zhang, R., Zhoa, H., Cai, H., Gush, K.A., Kerr, R.G., Pettit, G.R., Kraft, A.S., 1996. Preclinical pharmacology of the natural product anticancer agent bryostatin 1, an activator of protein kinase C. Cancer Res. 56, 802–808.